We are IntechOpen, the world's leading publisher of Open Access books Built by scientists, for scientists

4,800
Open access books available

122,000
International authors and editors

135M
Downloads

Our authors are among the

154
Countries delivered to

TOP 1%
most cited scientists

12.2%
Contributors from top 500 universities

CLARIVATE ANALYTICS BOOK CITATION INDEX INDEXED

WEB OF SCIENCE™

Selection of our books indexed in the Book Citation Index in Web of Science™ Core Collection (BKCI)

Interested in publishing with us?
Contact book.department@intechopen.com

Numbers displayed above are based on latest data collected.
For more information visit www.intechopen.com

5

Prospects for Neuroprosthetics: Flexible Microelectrode Arrays with Polymer Conductors

Axel Blau
Department of Neuroscience and Brain Technologies,
Italian Institute of Technology, Genoa,
Italy

1. Introduction

Neural prostheses are devices that interface with the central or peripheral nervous system. They target at the capture, modulation or elicitation of neural activity, in most cases to record the information flow within a neural pathway for its online or later decoding, or to mimic or replace neural functionality that has been compromised or lost. While in theory any information carrying modality of the neuron could be tapped into (*e.g.*, concentrations of neurotransmitters in the synaptic cleft, of energy carriers such as ATP or glucose, or of ions or oxygen; optical properties; ionic currents; membrane potential), most devices sample or alter the membrane potential (or a proportional quantity[1] thereto). Since the discovery and description of 'body electricity' by Luigi Galvani and Alessandro Volta in their studies on voltage-induced muscle contraction (Volta, 1793), metal electrodes have been used for establishing a bidirectional communication link between electrically excitable cells[2] and stimulation or recording apparatuses. From an engineering point of view, this has always been the least challenging and technologically least demanding approach. It just requires bringing a locally deinsulated conductor into close vicinity of a neuron to capture or induce fluctuations in its surrounding electrical field. Given the multitude of conductive materials to choose from and the ever growing number of technological possibilities for their structuring and processing into any desired shape and arrangement, historically, the interface of choice for neuroprosthetics has become the electrode array despite some of its fundamental conceptional shortcomings[3]. It has evolved into other clinically relevant

[1] Theoretically, any physical variable correlated to the membrane potential may be measured or altered. In a static scenario (*e.g.*, resting potential) it could be the electrical field, in a dynamic scenario (*e.g.*, upon de- or repolarization) its fluctuations, the (ionic) current(s) or even changes in the local magnetic field.

[2] Electrogenic cells in animals are neurons, muscle cells, pancreatic α- and β-cells, kidney fibroblasts or electroplaques. Besides the light-induced electron separation process during photosynthesis in plants, some microorganisms and algae are capable of electrogenesis as well (Logan, 2009; Rabaey & Rozendal, 2010).

[3] The electrical field at an electrode site is usually quite distorted due to the non-homogeneity of the biological environment in its vicinity. This does not only complicate signal source analysis in neural recordings, but it also limits the spatial precision with which neurons can be stimulated electrically. Even worse, if an electrical stimulus triggers an action potential in an axon, it may spread in both directions (towards the synaptic arbor and the soma), which is not observed in natural neural activity propagation.

readout derivatives such as electroencephalography (EEG), electromyography (EMG), electrocorticography (ECoG), and electroretinography (ERG). And it is still competitive with technologies making use of different recording or stimulation principles such as magnetic resonance imaging (MRI), magnetoencephalography (MEG), positron emission tomography (PET) or transcranial magnetic stimulation (TMS) (Clark, 1998; Lapitska *et al.*, 2009).

This chapter will review recent design trends for microelectrode arrays (MEAs) with an emphasis on flexible polymer devices, which may be exploited for neuroprosthetics. A brief synopsis on the history of *in vitro* and *in vivo* interfacing concepts with electrogenic cells introduces the chapter, followed by a discussion on their performance and limitations, to then take a look at latest strategies to overcome these limitations by resorting to new concepts, materials, and fabrication and modification processes. The chapter will conclude with the presentation and discussion of an innovative, versatile, and easy fabrication route for turning microchannel scaffolds into all-polymer neuroprosthetic electrode arrays. This strategy bears the potential of implementing a variety of secondary functionalities such as microfluidics, drug release schemes and optical stimulation paradigms, which may be operated in parallel to electrical recording and stimulation.

1.1 *In vitro* microelectrode arrays

To better understand the events at the cell-electrode interface, a variety of MEAs for the *in vitro* study of electrogenic cells have been developed over the past 40 years (Pine, 2006). Because they do not penetrate the cell membrane, they are considered 'noninvasive'. They sample local fluctuations of the electrical field generated by the membrane potential. Thus, any change in membrane potential due to a local and selective flux of specific ions (mostly Na^+ and K^+) across the cell membrane will lead to a capacitively mediated shift of charges in a nearby conductor (Butt *et al.*, 2003) or at the gate of a field effect transistors (FET) (Fromherz *et al.*, 1991; Fromherz, 2006; Poghossian *et al.*, 2009; Lambacher *et al.*, 2011). While FETs are restricted to the sampling of these events, metals or semiconductors can also be used for actively modifying them. By charging the electrodes (or more

Abbreviations: A/D, analog-to-digital; AP, action potential; APS, active pixel sensor; ASIC, application specific integrated circuit; CMOS, complementary metal oxide semiconductor; CNT, carbon nanotube; CP, conducting polymer; CPFET, cell-potential field-effect transistor; CSC, charge storage capacity; CT, computer tomography; CV, cyclic voltammetry; D/A, digital-to-analog; DIV, days in vitro; DRIE, deep reactive ion etching; ECoG, electrocorticography; EEG, electroencephalography; EGEFET, extended gate electrode field-effect transistor; EMG, electromyography; EOSFET, electrolyte oxide semiconductor field-effect transistor; ERG, electroretinography; FET, field-effect transistor; GND, ground (electrode); HMDS, hexamethyldisilazane; ITO, indium tin oxide; ISFET, ion-sensitive field-effect transistor; LCP, liquid crystal polymer; LFP, local field potential; LIGA, Lithographie, Galvanoformung, Abformung; MEA, microelectrode array; MEG, magnetoencephalography; MOSFET, metal-oxide-semiconductor field-effect transistor; MRI, magnetic resonance imaging; MTM, metal transfer micromolding; NCAM, neural cell adhesion molecule; NGF, nerve growth factor; NW, nanowire; PDMS, poly(dimethylsiloxane); PEDOT, poly(3,4-ethylenedioxythiophene); PFOCTS, trichloro(1H,1H,2H,2H-perfluorooctyl)silane; PET, positron emission tomography; PI, polyimide, PMMA, poly(methyl methacrylate); PPX, poly(p-xylylenes); PPy, poly(pyrrole); PS, poly(styrene); PTFE, poly(tetrafluoroethylene); PU, poly(urethane); PVA, poly(vinyl alcohol); S/N, signal-to-noise ratio; SAM, self-assembling monolayer; TMS, transcranial magnetic stimulation; VLSI, very-large-scale integration.

generally speaking, the interface), such capacitive shift can thus be imposed onto the cell membrane[5], which leads to a shift in its membrane potential and may result in the opening of voltage-gated ion channels (Bear *et al.*, 2007). Such arrays are used to find physiologically 'meaningful' electrical communication parameters, to study the influence of electrode topography or (bio-)chemical functionalization on cellular events, and to characterize the physiologically induced changes of such interface over time. In most cases, they are compatible with a majority of microscopy techniques for simultaneous morphology studies or the optical screening of membrane potential-associated variables (*e.g.*, by potential sensitive dyes or by imaging intrinsic changes of the optical properties of a cell, *e.g.*, its refractive index) or activity-associated events (*e.g.*, by calcium imaging). They are furthermore accessible to manipulation techniques such as drug delivery in pharmacological and toxicity assays (Gross *et al.*, 1997; Johnstone *et al.*, 2010), mechanical or laser microdissection in regeneration studies, or optical tweezers for biomechanical manipulation and force spectroscopy (Difato *et al.*, 2011). While an *in vitro* system may not truthfully reproduce the conditions of an *in vivo* environment and the events therein, MEAs have nevertheless been widely adopted for screening studies. They have become a tool and test bed for better understanding the design requirements (*e.g.*, material properties, coatings) of neural probes. Table 1 lists pioneering works and currently active groups or companies that have developed or commercialized key MEA technologies. Light-addressable devices were omitted (Bucher *et al.*, 2001; Stein *et al.*, 2004; Starovoytov *et al.*, 2005; Suzurikawa *et al.*, 2006). The terminology 'passive devices' refers to substrates with microelectrodes, tracks and connection pads that need to be connected to external amplification and signal processing hardware. 'Active devices' carry some of these electronics on-chip (Hierlemann *et al.*, 2011). In 'hybrid' devices, MEAs and signal conditioning electronics are produced separately but packaged together into a standalone device. They can furthermore include other types of electrochemical sensors on-chip (*e.g.*, for temperature, oxygen, pH, impedance, ...).

'Passive' MEAs	# of electr. *R: recording* *S: stimulation*	Device type and electrode materials
C.A. Thomas et al.	30	Two rows of 7 μm^2 electroplated Pt on Au/Ni electrodes on glass, insulated by photoresist (Thomas *et al.*, 1972)
G. Gross et al.	36 R,S 64 R,S	Ø 10 µm Au-coated ITO tracks on glass, insulated with a thermosetting polymer (Gross *et al.*, 1977; Gross *et al.*, 1985)
J. Pine	32 R,S	Two rows of sixteen 10 μm^2 electrodeposited Pt electrodes on Au tracks on glass, insulated by SiO_2 (Pine, 1980)

[5] The lipid double layer, which constitutes the cell membrane, can be considered a dielectric. The membrane thus acts as a capacitor that has no metal plates. Nevertheless, ions from the intra- and extracellular environments just accumulate at the (at physiological pH) negatively charged hydrophilic headgroups of the phospholipids at both sides of the membrane. If, as for most cells, the intra- and extracellular ionic compositions are different, a potential will build up across the membrane. As with any interface, the distribution of ions will very likely not be homogeneous but, to a first approximation, resemble a Helmholtz layer (Butt *et al.*, 2003). Thus, any additional charges (such as those at the surface of a metal electrode), which create an electrical field gradient in the vicinity of the membrane, will lead to a reorganization of these two electric double layers. Due to the difference in their distances from the electrode, this reorganization will affect the intracellular membrane interface less strongly than the extracellular membrane interface.

'Passive' MEAs (continued)	# of electr. *R: recording S: stimulation*	Device type and electrode materials
D.A. Israel *D.J. Edell* *R.G. Mark et al.*	25 R + 6 S	15 x 15 μm^2 electroplatinized, e-beam evaporated Au on Cr recording electrodes and 40 x 40 to 120 x 120 μm^2 stimulation electrodes on a Ø 40 mm glass coverslip, insulated by photoresist. Ultrasonically welded Au wires Ø 76 µm connection to miniature connector (Israel *et al.*, 1984)
J. Novac *S.A. Boppart* *K. Musick* *B.C. Wheeler et al.*	32 R,S 32 R,(S) 58 R,S	Ø 10 (25) µm Au/Ti on glass electrodes insulated by polyimide (Novak & Wheeler, 1986; Novak & Wheeler, 1988; Musick *et al.*, 2009) Ø 13 and 15 µm electroplatinized Au/Ti electrodes on perforated polyimide, insulated by polyimide (Boppart *et al.*, 1992) Ø 25 µm Au/Ti electrodes on SU-8 above microfluidic PDMS channels on glass (Musick *et al.*, 2009)
P. Connolly *L.J. Breckenridge* *R.J. Wilson* *M. Sandison* *A. Curtis* *C.D.W. Wilkinson et al.*	64 R,S	10 x 10 μm^2 or Ø 25 - 30 µm electroplatinized Au on NiCr electrodes on 125 µm thick polyimide insulated by polyimide (Connolly *et al.*, 1990; Breckenridge *et al.*, 1995; Sandison *et al.*, 2002)
Multi Channel Systems & NMI *H. Hämmerle* *M. Janders* *J. Held* *A. Stett* *W. Nisch et al.*	24, 36, 72 R,S flex 54, 60 R,S 32 R+12 S 256 R,S 60 R,S (3D)	Ti (or Au/Cr) tracks with TiN- or Pt- coated electrodes (usually Ø 10 or 30 µm) on glass or Au or Ti tracks with Au or TiN electrodes on (perforated) polyimide insulated by Si_3N_4 or polyimide (Haemmerle *et al.*, 1994; Nisch *et al.*, 1994; Janders *et al.*, 1996; Fejtl *et al.*, 2006) TiN-coated Ø 30 µm, 10 – 50 µm high electrodeposited Au/Ti pillar electrodes on glass insulated by Si_3N_4 (Held, Heynen*, et al.*, 2010)
P. Thiébaud *Y. Dupont* *L. Stoppini et al.*	6 R 34 R,(S) (3D)	10 x 10 μm^2 Pt on Ta electrodes with electroplated Pt (Ø 35 µm) on a perforated $Si/SiO_2/Si_3N_4$ substrate insulated by Si_3N_4 (Thiébaud *et al.*, 1997) 47 µm high, 15 µm exposed vapor-deposited Pt-tip on Ta electrodes on a porous (35%) Si substrate insulated by Si_3N_4 (Thiebaud *et al.*, 1999)
D. Hakkoum *S. Duport* *D. Muller* *P. Corrèges* *L. Stoppini et al.*	30 R,S 28 R,S	1.3 – 3.2 mm long, 15 µm wide Au/Cu on perforated polyimide (Upilex/Kapton) film (Stoppini *et al.*, 1997) 50 x 100 μm^2 electroplated Au on Cu/Ni on polyimide (Kapton®) with 5 perfusion holes (Duport *et al.*, 1999)
Y. Jimbo *A. Kawana*	64 R,S	Electroplated Pt-black on 50 x 50 μm^2 ITO tracks on glass insulated by a silicone photoresist (Kawana & Jimbo, 1999)
Alpha MED Scientific *H. Oka* *M. Taketani et al.*	64 R,S	50 x 50 μm^2 Au/Ni or 20 x 20 μm^2, 50 x 50 μm^2 or Ø 50 to 70 µm electrodeposited Pt-black electrodes on ITO tracks on a glass carrier insulated by polyimide or polyacrylamide (Oka *et al.*, 1999)
Ayanda Biosystems *M. Heuschkel et al.*	60 R,S (3D)	Pt, Au or ITO tracks with Pt or Au electrodes on glass; spike-shaped electrodes are available; SU-8 insulator (Heuschkel *et al.*, 2002; Heuschkel *et al.*, 2006)
C.D. James *J.N. Turner et al.*	124 R	24 x 5 + 4 electroplatinized Au/Ti electrodes (Ø < 10 µm) on fused silica wafer with $SiO_2/Si_3N_4/SiO_2$ insulation stack (James *et al.*, 2004)
F. Morin *Y. Takamura* *E. Tamiya et al.*	64	50 x 50 μm^2 Au/Cr electrodes on glass, insulated by "spin-on-glass" or photopatternable silicone (Morin *et al.*, 2005; Morin *et al.*, 2006)
L. Berdondini et al.	60 R,S	Ø 22 – 30 µm vapor-deposited Pt/Ti on Pyrex glass or Si, insulated by Si_3N_4; some are spatially partitioned by 5 interconnected clustering wells (Ø 3 mm in SU-8) (Berdondini *et al.*, 2006; Berdondini, Massobrio*, et al.*, 2009)
G. Gholmieh *T.W. Berger et al.*	39R+49S 60 R 64 R	ITO tracks with Ø 28 - 36 µm or 36 x 36 μm^2 Au- or Pt-coated electrodes on glass in a tissue-"conformal" arrangement, insulated by Si_3N_4 or SU-8 (Gholmieh *et al.*, 2006)

'Passive' MEAs (continued)	# of electr. *R: recording S: stimulation*	Device type and electrode materials
L. Giovangrandi G.T.A. Kovacs et al.	36 R,S	Ø 75 or 100 µm electroless Au-plated Ni/Cu electrodes on polyimide (Kapton®) insulated by an acrylic adhesive and polyimide (Giovangrandi *et al.*, 2006)
S. Rajaraman M.G. Allen et al.	12 – 13 R (3D)	Laser scribed, electroplated Ni/Cu/Pt-black electrodes (Ø < 10 µm) on a SU-8 microtower (fluidic) structure (< 500 µm height) on perforated fused silica insulated by parylene (Rajaraman *et al.*, 2007)
	25 R (spike, 3D) + 25 R (planar)	300 – 500 µm high, Ø 50 µm Au/Cr spike-tip or Ø 50 µm Au planar electrodes through metal transfer micromolding (MTM) in PDMS on SU-8, PMMA, or PU carrier with parylene insulator either selectively laser- and globally RIE- (CHF_3/O_2 plasma) deinsulated at the electrode sites, or applied during "capping protection" of the electrode sites. Pt-black plating (Rajaraman *et al.*, 2011)
J. Held O. Paul et al.	64 S,R	Pt/TiW on < 10 µm high, µm Ø Ag or sub-µm Ø Si (electroporation) microneedles on Si insulated by Si_3N_4 (Held *et al.*, 2008; Held, Gaspar, *et al.*, 2010)
S. Eick B. Hofmann	64 R,(S)	Ø 10 – 100 µm Au/Ti electrodes on glass sputtered with IrO_x with SiO_2, Si_3N_4, SiO_2 insulation sandwich (Eick *et al.*, 2009)
A. Offenhäusser B. Wolfrum et al.	30 R,(S)	Ø 3-5 µm apertures above Au/Ti electrodes on Si/SiO_2 with a SiO_2, Si_3N_4 insulator stack (Hofmann *et al.*, 2011)
G. Gabriel M. Bongard E. Fernandez R. Villa et al.	16 or 54 R,(S) + 2 GND	Drop cast CNT-decorated Ø 30 - 40 µm Pt/Ti recording and 2500 µm x 1000 µm GND electrodes (hexagonally arranged) on glass insulated by SiO_2, Si_3N_4 (Gabriel *et al.*, 2009; Bongard *et al.*, 2010)
A. Hai J. Shappir M. Spira et al.	62 R (3D)	Spine-shaped gold protrusions, electroplated on patterned Cu on glass, insulated by a $SiC/Si_3N_4/SiO_2$ stack (Hai *et al.*, 2009; Hai *et al.*, 2010)
F.T. Jaber F.H. Labeeda M.P. Hughes	16	40 x 40 μm^2 Au/Ti electrodes on glass and 20 x 20 μm^2 SU-8 microwells and interconnecting micro-trenches; SU-8 insulation layer (Jaber *et al.*, 2009)
P. Wei P. Ziaie et al.	4 - 16 (R),S	Ø 250 µm Au-coated nail-head pins and liquid Ga/In (75.5/24.5) tracks in PDMS microchannels (Wei *et al.*, 2009; Ziaie, 2009)
Axion BioSystems *J. Ross M.G. Allen B. Wheeler et al.*	64 R,S + 2 S (6 - 768 R,S)	Ø 30 µm Pt-black or Au/Ti electrodes on glass insulated by SU-8 or SiO_2 (Ross *et al.*, 2010)
P.J. Koester S.M. Buehler W. Baumann J. Gimsa et al.	52 R + 2 GND	Ø 35 µm Pt electrodes with interdigitated electrodes and PT1000 T sensor on glass insulated by Si_3N_4 (Koester *et al.*, 2010)
S.P. Lacour E. Tarte B. Morrison III et al.	20 R,S	30-75 x 100 μm^2 Au/Cr electrodes on deformable polyimide or PDMS with photo-patternable polyimide or PDMS insulator (Lacour *et al.*, 2010)
T. Ryynänen J. Lekkala et al.	60 R,(S)	Ø 30 µm Ti electrodes on glass insulated by polystyrene (PS) on hexamethyldisilazane (HMDS) (Ryynänen *et al.*, 2010)
W. Tonomura Y. Jimbo S. Konishi et al.	64 R	Electroplated Pt-black on Ø 30 µm Pt/Ti electrodes with Ø 5 or 10 µm substrate through-holes on backside-thinned Si/SiO_2 carrier with microchannels insulated by parylene-C (Tonomura *et al.*, 2010)
'Active' MEAs	# of electr. *R: recording S: stimulation*	Device type and electrode materials
A. Offenhäusser W. Knoll et al.	16 R 64 R	28 x 12 μm^2 and 10 x 4 μm^2 p-channel electrolyte oxide semiconductor FETs (EOSFETs) or Ø 30 - 60 µm extended gate electrode FETs (EGEFETs) insulated by Si_3N_4 (Offenhäusser *et al.*, 1997; Offenhäusser & Knoll, 2001)

'Active' MEAs (continued)	# of electr. *R: recording S: stimulation*	Device type and electrode materials
B.D. DeBusschere G.T.A. Kovacs	128 R	2 x 4 arrays of 16 Ø 10 µm Au/TiW/Al electrodes on CMOS IC, insulated by Si_3N_4 (Debusschere & Kovacs, 2001)
P. Bonifazi M. Hutzler A. Lambacher P. Fromherz et al.	4 - 16,384 R	Electrolyte-oxide semiconductor field-effect transistors (EOSFETs) with Ø 4.5 µm charge-sensitive spots at a density of 16000/mm^2 on silicon chips or multitransistor arrays (MTAs) based on metal-oxide-semiconductor field-effect transistor (MOSFET) technology (Bonifazi & Fromherz, 2002; Hutzler *et al.*, 2006; Lambacher *et al.,* 2011)
F. Patolskiy B. Timko B. Tian T. Cohen-Karni C. Lieber et al.	≤ 150 R,(S)	Straight or kinked, oriented p- and/or n-type Ø 20 nm silicon nanowires (SiNW) spanning about 2-5 µm between Ni (source and drain) or Cr/Pd/Cr metal interconnects insulated by Si_3N_4 or PMMA (Patolsky *et al.*, 2006; Tian *et al.*, 2010)
3Brain *K. Imfeld A. Maccione L. Berdondini et al.*	4096 R	CMOS APS with 21 x 21 µm^2 Al electrodes with optional Au-coating (electroless deposition) (Imfeld *et al.*, 2007; Berdondini, Imfeld*, et al.*, 2009)
F. Heer U. Frey A. Hierlemann et al.	128 R,S 126 R,S out of 11,011	8 x 16 array in CMOS technology with shifted Ø 10 - 40 (30) µm Pt-black (electrodeposited) on Pt (sputtered) electrodes insulated by an alternating Si_3N_4/SiO_2 stack (Heer *et al.*, 2007) 128 x 128 array of Ø 7 µm shifted Pt (sputtered) electrodes at a density of 3150/mm^2 on switch-matrix array in CMOS technology insulated by an alternating Si_3N_4/SiO_2 stack (Frey *et al.*, 2010)
J.F. Eschermann S. Ingebrandt A. Offenhäusser et al.	16 R	4 x 4 recording sites each with 6 parallel silicon nanowire (SiNW) FETs with widths of 500 nm and pitch of 200 µm on metalized, doped Si source/drain contacts insulated by SiO_2 (Eschermann *et al.*, 2009)
T. Pui P. Chen et al.	100 R	100 µm long silicon nanowires (SiNWs) with 30 x 40 nm^2 rectangular cross section attached to Al on Si contact pads insulated by Si_3N_4 (Pui *et al.*, 2009)
Z&L Creative Corp.	24 R	CMOS with Au-coated Al electrodes (Xin *et al.*, 2009)
'Hybrid' MEAs		
J.J. Pancrazio G.T.A. Kovaces A. Stenger et al.	32 R,S + 4 GND	Electrochemically platinized Ø 14 µm Au/Cr electrodes on Si/SiO_2 carrier connected to a CMOS/VLSI amplifier chip, insulated by Si_3N_4 (Pancrazio *et al.,* 1998)
Bionas GmbH *W. Baumann R. Ehret M. Brischwein B. Wolf et al.*		Multiparametric sensor with 6 µm^2 CPFET and Ø 10 µm Pd or Pt electrodes, ISFET pH electrode, interdigitated impedance electrodes, photodiodes, oxygen and T sensor (Baumann *et al.*, 1999; Ehret *et al.*, 2001; Baumann *et al.*, 2002)
W. Cunningham D. Gunning K. Mathieson A.M. Litke M. Rahman et al.	61 R,S 512 R,S 519 R,S 61 R,S (3D)	Ø 2 - 5 µm electroplated Pt electrodes on ITO on glass, insulated by Si_3N_4, wire-bonded to ASIC readout & stimulation circuitry (Cunningham *et al.*, 2001; Mathieson *et al.*, 2004) Hexagonally arranged, ≤ 200 µm high, partially hollow W needles with electroplated Pt-tips, insulated by SiO_2 and back-side connected to Al tracks, wire-bonded to ASIC readout & stimulation circuitry (Gunning *et al.*, 2010)

Table 1. List of groups and companies that have developed a particular MEA technology[6] sorted by first publication date, then author. Apologies go to any group or technology accidentally omitted or cited wrongly. Consult second page of chapter for abbreviations.

1.2 From *in vitro* to *in vivo*

From a conceptual point of view, the readout and stimulation physics of *in vitro* electrode systems are identical to electrode-based *in vivo* probes. Also, the needs for amplification,

[6] News on technological developments may be found on the continuously updated publication list on Multi Channel Systems' website.

filtering, analog-to-digital (A/D) signal conversion and signal (post-) processing electronics are almost the same. This holds for signal readout circuitry on the one hand, and for signal generators and digital-to-analog (D/A) converters for modulating neural activity with electrical stimuli on the other hand. It does not matter whether they are placed in direct vicinity of the electrodes as in recent 'active' MEA designs, or classically connected as modular hardware at the end of the electrode tracks of 'passive' MEAs. A comprehensive review by Jochum *et al.* surveys neural amplifiers with an emphasis on integrated circuit designs (Jochum *et al.*, 2009).

Yet, *in vivo*, new challenges arise. The electrode array encounters a rather different and more complex environment when compared to *in vitro* scenarios. Any array cannot longer be considered 'noninvasive', even if it will not penetrate the cell membrane. This is because a MEA has to be brought first into its recording position, which involves the opening and partial removal of the skull and of any protective encapsulation of the brain. Deep brain implants need to be furthermore inserted into the soft, yet densely packed brain tissue, thereby, in the best case, just displacing, and in the worst case, even destroying neurons, connections and glia cells along the penetration path. This may lead to a partial destruction of the tissue architecture, which the brain needs to compensate for. Apart from the insertion damage, a rigid neural implant may get repositioned upon a sudden movement of the head due to the inertial forces acting on the quasi-floating brain. Furthermore, the immune system may become activated and attack the implanted portion of a device. The implant materials are thereby exposed to a variety of compounds not found in *in vitro* systems that they may chemically react with. In bad scenarios, the reaction products may be toxic, thereby triggering a temporary if not chronic immune response[7]. Any change of the device material may furthermore be categorized as 'degradation', which could compromise device stability and performance over time. The latter may also be simply lowered by device encapsulation in tissue scars, thereby electrically insulating the recording and stimulation sites. This scarring is considered as one of the most common reasons for device failure. Stimulation electrodes carry additional risks of tissue damage by their electrochemical erosion or overheating (Dowling, 2008; Marin & Fernandez, 2010). In summary, implant materials should be chosen that are sufficiently biostable against alterations or degradation by the physiological environment. They should furthermore not trigger any immune response or alter cell physiology in an uncontrolled and undesirable fashion[8]. In other words, a neuroprosthetic recording device should behave as if it were not present, and a stimulation device should in addition induce a neural response as similar to neural signaling mechanisms as possible.

Another critical issue is the actual interconnection of the devices to the outside world. Signals are commonly transferred to extracorporeal signal conditioning and processing electronics by cables. Not only are the connection points between cable and device a source of failure due to the detachment of the cable ends to the device by chemical degradation or mechanical forces. Once passing through the skin or skull, the pass-through hole has to be well sealed and stabilized to not let contaminants pass and become a site of chronic infection, and to not let the cables move and thereby exert mechanical stress onto the surrounding tissue. Recent trends therefore target at the transmission of signals through the

[7] Apart from reaction products stemming from device degradation, exposed implant materials may also have catalytic properties.

[8] This statement does not exclude the temporary or permanent chemical and/or topographical device functionalization for manipulating or triggering a cell or tissue response in a controlled way (*e.g.*, to support device – tissue integration or tissue regeneration).

skull by telemetric technologies, which, however, pose new challenges with respect to miniaturization, circuit protection against humidity, and energy transfer for powering the telemetric electronics. And it does not provide a solution for stabilizing the internal circuit-to-MEA connection, which may still be exposed to movement-related stress.

1.3 Electrode arrays for *in vivo* electrophysiology

For getting a general overview on *in vivo* neuroprosthetic[9] implants and brain-machine interfaces including the diverse types of microelectrode arrays, their specific applications and main vendors, the reader shall be referred to recent overview articles and reviews (Hetke & Anderson, 2002; Rutten, 2002; Navarro *et al.*, 2005; Cheung, 2007; Winter *et al.*, 2007; Dowling, 2008; Hajjhassan *et al.*, 2008; Lebedev *et al.*, 2008; Wise *et al.*, 2008; Stieglitz *et al.*, 2009; Graimann *et al.*, 2010; Mussa-Ivaldi *et al.*, 2010; Rothschild, 2010; Hassler *et al.*, 2011). This paragraph will just summarize some of the basic design concepts, general fabrication approaches and the limitations they impose on the performance of chronically implanted devices.

1.3.1 Design and fabrication aspects

In the 80's of the last century, the boom in microfabrication technologies opened the door for designing elaborate multi-microelectrode arrays with spatially distributed recording or stimulation sites. However, the choice of carrier, conductor and insulator materials depends on (and is thereby limited by) the often harsh fabrication and processing conditions. Given that materials in tissue-contact also need to fulfill the condition of being biocompatible (that is foremost, not being cytotoxic) and biostable (that is, not become degraded by the physiological environment), the number of suitable materials is quite low. Almost all of them are considerably more rigid than soft tissue, and the devices made from them tend to have sharp edges. Anyone ever having experienced a splinter in the thumb will remember how painful[10] it is each time the splinter moves only the tiniest bit. The simple reason is: the splinter is rigid and edgy whereas the tissue of the thumb is not. Thus, despite the tremendous research investments into diverse neuroprosthetic technologies, intracortical probes still lack functional stability during chronic use due to the large discrepancy between their biomechanical and chemical properties and those of the tissue environment (Marin & Fernandez, 2010).

The need for designing more flexible electrode arrays was already addressed in the 60's of the last century (Rutledge & Duncan, 1966). Various strategies have been suggested since then to overcome some of the above mentioned limitations, particularly in the context of designing cochlear, retinal and deep brain implants. Today, the most commonly used flexible carrier and track insulation materials are polyimides (PIs), poly(p-xylylene) (PPX, and in particular poly(chloro-p-xylylene) (Parylene®-C)), poly(dimethylsiloxane) (PDMS), poly(tetrafluoroethylene) (PTFE), and occasionally less flexible liquid crystal polymers (LCPs) or photoresists (*e.g.*, SU-8) (Navarro *et al.*, 2005; Cheung, 2007; Myllymaa *et al.*, 2009; Hassler *et al.*, 2011). Noble metals[11] such as Pt, Ir, W and Au are sputter- or vapor-deposited, often requiring other metals (*e.g.*, Ti, Cr) as adhesion promoters. They are structured into electrodes, tracks and connection pads by etching through a sacrificial mask of photoresist, glass or metals

[9] The most well-known neuroprosthetic devices are cochlear implants, retinal implants, spinal cord stimulators, deep brain implants and bladder control implants.

[10] While the brain processes information on pain in other body parts, it does not feel pain itself.

[11] Sometimes less noble metals like Ni or Cu are used as track and connection pad conductors. If the insulation layer of the probe has defects, they may partially dissolve into cytotoxic ionic species.

(Patrick *et al.*, 2006; Wang *et al.*, 2007; Mercanzini *et al.*, 2008; Rodger *et al.*, 2008). With few exceptions, each device needs to be fabricated in a clean room environment. Only recently, new strategies have been proposed to microstructure conductors under normal laboratory conditions that allow their transfer onto or embedding into polymer carriers that do not withstand high temperatures or vacuum. Hu *et al.* first sintered metal nanopowders within micropatterned, temperature-resistant multilevel microchannel quartz molds, which were then embedded into PDMS, parylene or polyimide. This allowed the generation of high-aspect (10:1) 3D conductors with, depending on the chosen mold generation process (ion milling, laser milling, deep reactive-ion etching (DRIE)), a wide variety of arbitrary shapes. A volume reduction between 5 % and 25% during sintering led to gaps between the conductor and the mold, which were filled with PDMS, thereby automatically insulating the tracks (Hu *et al.*, 2006). A different approach was chosen by Dupas-Bruzek and coworkers, which was based on the UV (248 nm) laser-assisted activation of PDMS followed by the electroless deposition of Pt onto the laser-treated and thereby chemically modified surface areas (Dupas-Bruzek, Drean, *et al.*, 2009; Dupas-Bruzek, Robbe, *et al.*, 2009). Henle *et al.* created a PDMS-Pt-PDMS sandwich by placing a 12.5 µm thin Pt film directly onto a partially cured PDMS carrier substrate, structuring it by an IR (1064 nm) laser, manually discarding excess material and spin-coating a second PDMS layer on top (Henle *et al.*, 2011). All of these fabrication approaches have in common that pads and electrodes get insulated during device fabrication and need to be reexposed in a post-processing step (*e.g.*, by laser deinsulation or etching). Furthermore, tracks, pads and electrodes are always made from metals. Often, their long-term performance is limited due to the delamination of insulation layers or material fatigue over time. And finally, even such flexible neural implants still contain parts that are either more rigid than the surrounding tissue or lack the arbitrary deformability to follow its shape.

We therefore decided to deviate from common microelectrode array fabrication paradigms by resorting to a microchannel replication strategy with conductive polymers (CPs) completely replacing metals. This does not only allow the implementation of one and the same electrode layout in different types of insulating polymer backbones (*e.g.*, of different shore hardness). It also gives more freedom in the choice of conductive materials that have biomechanical properties more similar to the embedding substrate. Fundamental proof-of-principle results have been published recently (Blau *et al.*, 2011). The concept is sketched out in Fig. 1. It exemplarily illustrates the master fabrication and the replica-molding routes for *in vitro polyMEA*s with or without spike electrodes on the one hand, and copies of the master on the other hand. The initial **m**aster with bi-level microstructures for electrodes, conductor tracks and contact pads can be made out of two SU-8 layers following standard photolithography recipes[12]. A silicon wafer (m1) is spin-coated with SU-8 (m2), which is then soft-baked and illuminated through a photo mask (m3) to create the features of all three elements, the electrodes, tracks and pads. After a post-exposure bake (m4), a second SU-8 layer is spun on top of the first and soft-baked (m5), then exposed through the carefully aligned second photo mask with electrode and pad features only (m6). Thereafter follows a standard post-exposure bake (m7) and the development of both layers (m8). The individual layer thicknesses can be controlled by the spin coating parameters to define separate heights for buried track channels and for scaffold-penetrating electrodes and pad wells, respectively. Although the one-time fabrication of the molding master may still

[12] Alternatively, arbitrary 3D shapes could be inscribed into a photo-patternable polymer when resorting to UV laser or multi-photon lithography. One of the advantages would be the direct generation of non-vertical (*e.g.*, conical) structures (Li & Fourkas, 2007; Thiel *et al.*, 2010).

require a clean room infrastructure[13], devices can be fabricated in a normal laboratory environment. In addition, a master can be replicated at negligible cost by the very same replica-molding procedure that is used to manufacture individual devices.

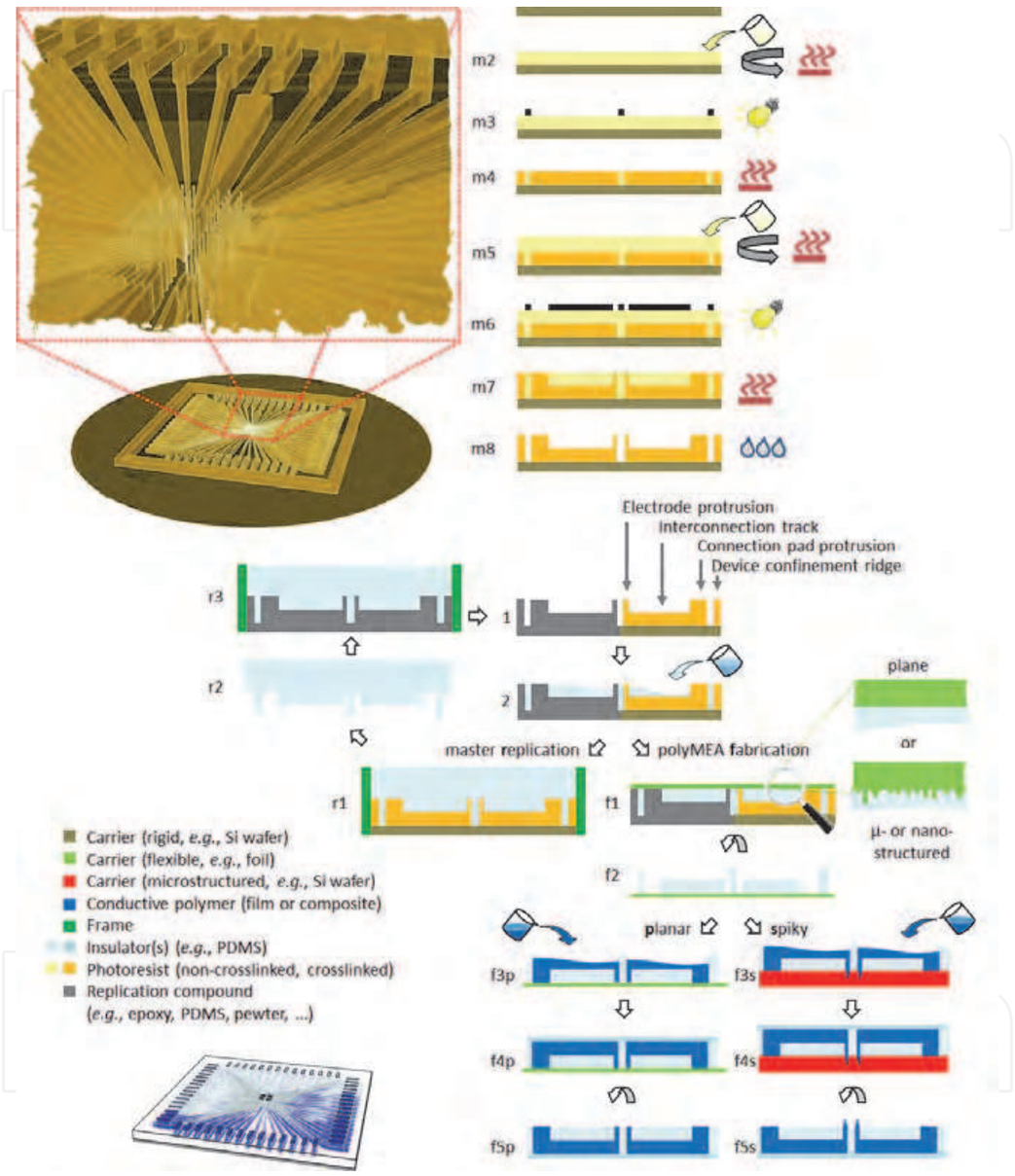

Fig. 1. Summary of the eight steps (**m1-m8**) for fabricating a bi-level replication **m**aster in SU-8 on a Si-wafer (upper left sketch with zoom onto the electrode columns), the three master-replication steps (**r1-r3**) and the five steps (**f1-f5**) for fabricating a *polyMEA* (lower left sketch). See text for details. Legend: **f**, device **f**abrication route; **m**, **m**aster production; **r**, master **r**eplication route; **p**, **p**lane electrodes; **s**, **s**pike electrodes.

[13] If device geometries are simple and dimensions stay above a few tens of microns, even the master can be fabricated in the laboratory, as demonstrated by several groups (*e.g.*, (Mensing *et al.*, 2005)).

The bi-level master (1, grey, orange) (*e.g.*, made of a high aspect ratio photoresist) is usually coated by an anti-adhesive film[14] before being filled with a curable polymer gel (2, sky blue) (*e.g.*, PDMS). Alternatively, the master (or a sturdier copy thereof) can be used for hot-embossing into a thermomoldable polymer. A plane or micro-/nanostructured (zoom in) sacrificial carrier foil (green) levels the polymer with the highest protrusions of the master (f1). This ensures the complete penetration of the polymer by the elevated structural features of the master. After the curing of the thin polymer microchannel scaffold, such carrier helps in scaffold removal from the master without running the risk of tearing it apart. It furthermore allows the purposeful imprinting of a topofunctional texture into the PDMS surface and/or the electrodes of a *polyMEA* (*e.g.*, for steering neural differentiation or guiding neurites). After flip over (f2), the carrier also temporarily supports the scaffold during the subsequent processing steps for generating a *polyMEA* with **p**lane electrodes (route **p**). To create the electrodes, tracks and pads, the microchannels and cavities of the scaffold are filled with the CP (f3p). If the CP wets the channel-separating plateaus in this step, it can be rather easily scraped off after partial evaporation of the solvent. After curing, the scaffold is backside-insulated by a second polymer layer (f4p). If a foil or panel is chosen as the insulator and a film-forming CP as the conductor, the channels stay hollow and can serve for microfluidic or optical add-on applications. In this case, the sizes of the electrodes are less well defined. On the top-side of the *polyMEA*, they will have ring shapes with a through-hole diameter and wall thickness equaling the film thickness of the CP rather than being planar. However, a neuron could partially get into contact with the CP-coated channel sidewalls upon entering the channel or sending any of its processes into the channel. Thus, theoretically, the entire channel surface will serve as an electrode. Alternatively, all cavities are filled with the same or a similar curable polymer gel from which the scaffold was made of. Depending on the stickiness of the temporary carrier foil, the disk-like CP depositions on the carrier at the electrode sites and contact pads are more likely to be transferred to the polymer rather than sticking to the carrier. This is because a dried CP film usually has a nano-structured surface that gets physically entrapped by the polymer gel insulator. This issue is discussed in the next paragraph in more detail. After removing the carrier[15], the *polyMEA* with planar electrodes (f5p) is ready for use. No other deinsulation step is required. If **s**pike electrodes shall be generated instead (route **s**), the scaffold is transferred onto a carrier with cone-like indentations (red), which can be generated by *e.g.*, anisotropic etching of Si (Jansen *et al.*, 1996; Williams & Muller, 1996) or multidirectional UV lithography in photoresist (Yong-Kyu *et al.*, 2006). After aligning those with the electrode through-holes of the scaffold, the CP can be filled into the cavities and cured (f3s). Rajaraman *et al.* recently presented a similar approach for pyramid-shaped metal electrodes

[14] To generate a Teflon®-like, fluorine-terminated anti-stick film, the wafer with the SU-8 microstructure or its epoxy copy can be either exposed for 5 minutes to C_4F_8 in a reactive ion etcher or to trichloro(1H,1H,2H,2H-perfluorooctyl)silane (PFOCTS) for one hour in a desiccator.

[15] One strategy to pull 50 - 200 µm thin PDMS microchannel scaffolds from their molding masters without tearing them apart was to place coated overhead or inkjet transparencies with their coated sides onto the uncured PDMS. In most cases, the water-soluble coating had a texture, which seemed to physically entrap the PDMS. After curing, the PDMS thus stuck to the sacrificial support transparency. It would detach from it automatically upon dissolution of the coating during immersion into water or ethanol for a few hours, leaving the texture topographies imprinted in the PDMS surface. As already briefly mentioned earlier, the transparency or its coating can be purposefully micro- or nanostructured to permanently transfer topographical cues into the PDMS and/or the CP electrodes.

(Rajaraman *et al.*, 2011). As before, a backside insulation layer is applied (f4s) to give a *polyMEA* with spike electrodes after its peeling from the microstructured carrier. The spikes can either be used as such or, if a small recording/stimulation site is desired, be insulated by a thin coat of PDMS and then be clipped at their tops (*e.g.*, by a razor-blade through a mask with holes) to expose the CP.

During the *polyMEA* fabrication steps sketched out in Fig. 1, the CP will always get into contact with the transfer carrier foil (green) at the pad and electrode openings in the scaffold. Depending on the surface structure and chemistry of the foil, film-forming CPs like PEDOT:PSS from aqueous dispersion might stick more or less well to it (Fig. 2, a1 & a2). Upon peeling the foil from hollow channels, the sub-µm-thick CP membrane spanning the electrode through-hole may get partially or completely torn off and/or stay stuck to the carrier foil (Fig. 2, a2, left channel). If, instead, CP-coated channels are backfilled with a polymer gel like PDMS, the gel will get mechanically entrapped in the CP film due to its roughness (on the nm scale) thereby acting as a mechanical support for the membrane after curing (Fig. 2, a2, right channel).

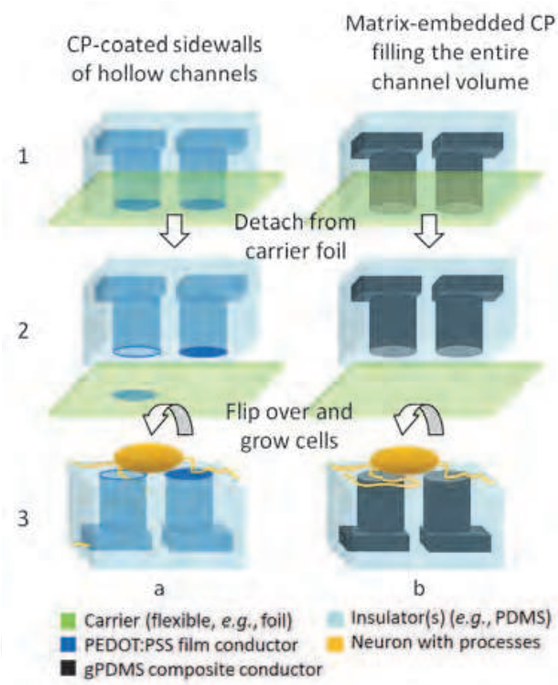

Fig. 2. Zoom onto a sketch of two electrode channels in contact with a transfer carrier to illustrate how different CPs give different types of electrodes.

Both scenarios give useful devices for different application needs. A neuron may just grow its processes into a CP-coated channel without electrode membrane (Fig. 2, a3, left channel). Thus, the recorded signal can be easily attributed to that very neuron. Alternatively, if the well diameter were reduced to a few µm, a planar-patch-like recording array could be created. As recently reported by Klemic *et al.* (Klemic *et al.*, 2005), Chen and Folch (Chen & Folch, 2006), Tonomura *et al.* (Tonomura *et al.*, 2010), and Hofmann *et al.* (Hofmann *et al.*, 2011), neurons tend to seal such microapertures to result in high signal-to-noise (S/N) ratios and selectivity. A back-filled channel with an intact electrode membrane (Fig. 2, a3, right

channel) or a gPDMS composite (Fig. 2, b1-3) will act like a classical electrode instead. Even if the CP membrane were missing, the electrode would be defined by the nm-thick ring-shaped CP coating at the end of a channel. It is still an open question whether the impedance of these ring electrodes is sufficiently low to capture or induce neural signals.

1.3.2 PDMS as a soft and flexible substrate material

The platinum-catalyzed addition-crosslinking of vinyl-endblocked silicone polymers and silicone polymers with SiH functionality gives medical grade polydimethylsiloxane (PDMS) (*e.g.*, Dow Corning, Sylgard 184; Wacker, Elastosil RT 601), a rubberlike polymer with particular properties (Colas & Curtis, 2004). Not only can a wide variety of different hardness and tear resistances be chosen from. It is furthermore dimensionally stable and will not shrink or expand upon curing. If not chemically activated (*e.g.*, by plasma oxygenation or other types of surface functionalization (Donzel *et al.*, 2001)), it reversibly adsorbs to almost any smooth surface but will not react with it. It demonstrates outstanding bioperformance and has a favorable toxicological profile in diverse medical contexts (Briquet *et al.*, 1996). It is therefore FDA-approved and part of common implants that are in direct tissue contact (*e.g.*, breast implants, contact lenses, tubing in heart surgery, catheters) (Colas, 2001; Curtis & Colas, 2004). It can furthermore be used as a molding material to cast itself[16] or various other materials such as plasters, concrete, wax, low-melt metal alloys (tin, pewter) or resins (urethane, epoxy or polyester) for master replication purposes (Smoothon, 2008). After depositing a conductive seed layer, it can also be electroplated to give LIGA-type master replicas (Jung *et al.*, 2008).

1.3.3 Flexible, polymer-based electrode materials

The desire of incorporating electronics into bendable and stretchable lightweight consumer devices (*e.g.*, rollable displays, garment, conformal solar panels) has driven the research and development of unconventional elastomeric conductors (Rogers *et al.*, 2010) including inks based on single-walled carbon nanotubes (Sekitani *et al.*, 2009) or silver nanoparticles (Ahn *et al.*, 2009). Despite their lower electrical conductivity (Kahol *et al.*, 2005), conductive polymers promise to become a low-cost alternative to metals for their flexibility and easier processability (Inganäs, 2010). Currently, PEDOT:PSS is one of the CPs with the highest conductivity, is transparent, forms bendable films, is chemically inert and non-cytotoxic. It has therefore found its way into the biosciences as a selective sensing layer in biosensors (Janata & Josowicz, 2003; Lange *et al.*, 2008; Rozlosnik, 2009) and more recently as a feature enhancer of metal microelectrodes (Guimard *et al.*, 2007; Widge *et al.*, 2007). Besides the two conductivity modes (electron-hole and ionic) of CPs, their biophysical properties and process-dependent micro- and nano-topographies seem to enhance their bio-acceptance and tissue integration (Ateh *et al.*, 2006; Guimard *et al.*, 2007; Owens & Malliaras, 2010).

While graphite and, in particular, carbon black are usually not categorized as polymers, they share some of their properties with respect to their extended carbon backbone. For their high electrical conductivity, biological inertness, low price and easy handling, they are excellent filler materials for creating flexible, voluminous conductor tracks or coatings with

[16] PDMS adheres strongly to itself. For a successful PDMS replication from a PDMS master, the master surface needs to be coated with an anti-stick layer. The one-hour exposure to trichloro(1H,1H,2H,2H-perfluorooctyl)silane (PFOCTS) in a desiccator results in a reusable Teflon®-like transferring layer (Zhang *et al.*, 2010).

silicones or polyurethanes as the matrix (Calixto *et al.*, 2007; Huang *et al.*, 2011). As with any conductive filler (*e.g.*, antimony- or indium-doped tin oxide, silver (Ahn *et al.*, 2009; Gong & Wen, 2009; Larmagnac *et al.*, 2010; Zhang *et al.*, 2011), carbon, or any form of their nanoparticle derivatives (Sekitani *et al.*, 2009; Pavesi *et al.*, 2011)), a conductive polymer can be generated when the percolation threshold[17] of the filler has been surpassed (Kirkpatrick, 1973; Milliken and Company, 1997). Rather than being a thin film conductor[18] such as PEDOT:PSS or most of the vapor-deposited metal electrodes, the composite fills the entire volume of the microchannel, thus being less prone to dramatic changes in its conductivity upon deformation[19]. As shown for other flexible wire composites (Ahn *et al.*, 2009), it is hypothesized that the main reason for the stability in conductivity of such flexible wires is the disperse distribution of graphite flakes in the PDMS. Upon shifting these flakes against each other, the current will just follow an alternative or even newly established conductive pathway between different flakes being or getting into contact with each other. Thus, by filling channels of extended dimensions with gPDMS, the shortcoming of its lower conductivity compared to metals can be partially compensated by its bulk-like distribution.

1.3.4 Electrode functionalization and post-processing strategies

The postprocessing of devices serves two main goals: i) the improvement of the electrical characteristics of the electrodes (mainly with respect to the decrease of their electrical impedances and/or the increase of their reversible charge delivery capacity (CDC)[20], and ii) the enhancement of their biocompatibility for their better tissue integration. The electrical impedance is a more general concept of electrical resistance; it describes the frequency-dependent resistance of an electrical conductor. At '0 Hz', the alternating current (AC) impedance of an electrode is identical to its direct current (DC) resistance. Over the physiologically relevant frequency range between 0.5 - 100 Hz (relevant for slow oscillations as in local field potentials (LFPs)) and 1 - 5 kHz (for the capture of individual action potentials (APs) of neurons[21]), the impedance of conductors can decrease by 2-3 orders of magnitude. In general, it can be stated that the smaller the geometrical electrode area (*e.g.*, πr^2 for disk-like electrodes with radius r), the higher the impedance. The impedance of a

[17] Percolation as a mathematical concept refers to the long-range connectivity and its nature in random systems. The percolation threshold is the critical value of the (volume) occupation probability where infinite connectivity, in this case between conductive particles, first occurs.

[18] The resistance of thin-film electrodes may considerably deviate by two to three orders of magnitude from that of the bulk conductor material (Hu *et al.*, 2006).

[19] Nevertheless, any wire deformation will alter the resistance of a wire. This phenomenon is exploited in strain gauge sensors. However, while the working principle of a strain gauge sensor relies on the mechanically induced changes in the cross-section geometry of the conductor, the resistivity of a composite material such as gPDMS seems to be dominated by the number of parallel conductive pathways. While the resistance in a strain gauge sensor increases with strain, the resistance of carbon- or silver-blended PDMS was actually found to decrease upon stretching for the better contact of the conductive particles (Niu *et al.*, 2007).

[20] Often, the reversible CDC is also referred to as the reversible charge storage capacity (CSC) or the save/reversible/capacitive charge injection limit (CIL).

[21] The reasoning is as follows: During the firing of an action potential, the depolarization of the cell membrane lasts for about 1-2 ms. The temporal width of the extracellularly recorded component of such action potential is usually 1 ms (or less). This translates into a theoretical frequency of 1 kHz (or above) because 1000 (or more) such components will fit into 1 s.

small-diameter electrode can be lowered by increasing its real (or effective) surface area, *e.g.*, by adding a microtopography to the electrode (*e.g.*, by increasing its roughness). Depending on the structure of that surface topography (*e.g.*, fractal or columnar) and the type and electrical properties of the material that creates it, the capacitance[22] C of the electrode may be affected as well. Decreasing the impedance will increase the signal-to-noise ratio and decrease the required voltage U to charge the electrode-electrolyte interface. Increasing the capacitance of the electrode gives room for more charges Q to accumulate on the electrode surface at a given voltage ($Q = C \cdot U$), thereby increasing the number of separated ionic charges at the electrode-electrolyte-tissue interface. Consequently, the increase in the locally generated electrical field may increase the likelihood of sufficiently shifting the membrane potential over its depolarization threshold in stimulation experiments[23]. The effect of decreasing electrode impedances by depositing non-planar metal layers (*e.g.*, porous Pt-black, columnar TiN or fine-grained IrO_x) has been exploited for a long time. A new trend is the deposition of carbon nanotubes (CNTs), which have favorable electrical and biophysical properties. They not only improve the impedance and the charge transfer capacity by more than one order of magnitude, but provide nano-textured anchoring points that cells can make use of (Keefer *et al.*, 2008; Park *et al.*, 2009; Malarkey & Parpura, 2010). Recent studies show the same effect for CPs. Ludwig *et al.* reported on an about 10-fold decrease in impedance at 1 kHz for electrochemically deposited PEDOT coatings on Ø 15 µm Au recording electrodes, which reduced noise levels by about half (Ludwig *et al.*, 2011). In earlier studies, the same effect was demonstrated for polypyrrole (PPy) (Cui *et al.*, 2001). Kotov *et al.* and Beattie *et al.* recently summarized the potential of nanomaterials for neural interfaces (Beattie *et al.*, 2009; Kotov *et al.*, 2009).

Many works have addressed the issue of providing signaling cues on electrode and substrate surfaces to mask the non-biological properties of a material, and to alleviate the acute and chronic disturbances imposed by a neuroprosthetic device onto its surrounding biological environment (Leach *et al.*, 2010). By adsorbing polycations onto ready-made CP layers (Collazos-Castro *et al.*, 2010) or by entrapping or intermingling cell adhesion and differentiation promoting proteins or their fragments (*e.g.*, neural cell adhesion molecules (NCAMs), nerve growth factor (NGF), laminin and fibronectin) into the CP during its

[22] In a first approximation, the electrode can be considered the plate of a parallel-plate capacitor. Its electrical capacitance C is then directly proportional to the real electrode surface area A, which is equal or bigger than the geometrical electrode area. ($C = \varepsilon \cdot A/d$, with the permittivity ε of the dielectric and the distance d between the plates). While the proportionality holds, the situation at the electrode-cell interface is certainly more complex: The second plate is not of the same type as the electrode but the cell membrane with a different surface area. Furthermore, the dielectric, the medium between electrode and cell membrane, is not static, and thus its permittivity is not a constant.

[23] Two types of currents are distinguished: Capacitive currents just charge the electrode; electrons will accumulate on the outer electrode surface without being injected into the electrolyte. Most stimulation electrodes are designed to be capacitive. In contrast, Faradaic currents pass the electrode-electrolyte interface. Because free electrons cannot be dissolved in aqueous environments, they become immediately involved in a redox-reaction. The occurrence of such undesirable reactions leads to chemical products that alter the composition of the physiological environment. To avoid any Faradaic currents, stimulation electrodes can be sealed by dielectric films (*e.g.*, TiO_2, Ta_2O_5 and $BaTiO_3$). They are generated by oxidizing the respective metal electrodes, sputtering, sol-gel deposition or precipitation from organic or water-based dispersions. For an in-depth discussion see (Merrill *et al.*, 2005; Cogan, 2008; Zhou & Greenberg, 2009; Merrill, 2010).

electrochemical or self-assembled monolayer (SAM) formation, it could be shown that brain-derived cells attached preferentially to the CP (Cui *et al.*, 2001; Widge *et al.*, 2007; Asplund *et al.*, 2010; Green *et al.*, 2010; Thompson *et al.*, 2010). Recent studies indicate that, apart from its overall geometry and surface chemistry, the nano and micro surface texture of a substrate may have considerable impact on cell adhesion, differentiation, cell morphology and gene expression as well (Wilkinson, 2004; Barr *et al.*, 2010). Depending on the type of starting material, the deposition parameters (temperature, pH, U, Q, time) and the choice of solvents and auxiliary components (such as surfactants), the form, texture and order of CPs can be fine-tuned (George *et al.*, 2005; Yang *et al.*, 2005; Abidian *et al.*, 2010). And since Wong *et al.* observed that the shape and growth of (endothelial) cells could be noninvasively controlled by just switching the oxidation state of fibronectin-coated PPy (Wong *et al.*, 1994), and that current flow through PPy would promote protein synthesis and neurite outgrowth (Schmidt *et al.*, 1997), later works exploited this combination of conductivity and particular geometries of CPs for the programmable control of *e.g.*, neurite extension, protein adsorption and cell adhesion, or for the spatially defined release of ions, antibiotics, anti-inflammatories, neurotransmitters and other signaling factors (Abidian *et al.*, 2010; Ravichandran *et al.*, 2010; Sirivisoot *et al.*, 2011; Svennersten *et al.*, 2011). While the roughening of electrodes and the incorporation of biofunctional cues in all cases provide mechanical and biochemical anchoring points for cells, CP coatings are lightweight and usually less brittle than metal deposits. Furthermore, unlike metals, both CNTs and CPs are chemically accessible to covalent pre- or post-modification with bioactive molecules (Ravichandran *et al.*, 2010).

1.3.5 Performance of *polyMEA* devices

The electrical, mechanical and optical characteristics as well as the recording performance of *in vitro polyMEA*s and epidural *in vivo* probes derived therefrom have been presented in a recent proof-of-concept study (Blau *et al.*, 2011). The main characteristics are summarized below. *polyMEA*s for *in vitro* applications were designed to fit the pin-layout of a commercial 60-channel amplifier system (Multi Channel Systems). Their overall dimensions of 4.9 x 4.9 cm^2 matched commercial MEAs. Their minimal thickness could not stay below the height of the bilayer master features, which were between 200 and 500 µm. To reach the standard height of 1 mm of commercial MEAs, either temporary spacers or a permanently fused PDMS backside insulation coat were used. Device flexibility depended on device thickness. With increasing thickness above 200 µm, the PDMS still stayed flexible but slowly lost its surface conformability. A *polyMEA* with gPDMS electrodes, tracks and pads of approximate thickness of 300 µm is depicted in Fig. 3a. Electrode diameters of the 8 x 8 (- 4 corner electrodes) electrode matrix were nominally 80 µm. Electrode spacing was 400 µm with the exception of an 800 µm cross-shaped gap in the center of the electrode matrix. Device transparency of a *polyMEA* with PEDOT:PSS conductive films and PDMS-flooded cavities is demonstrated in Fig. 3b & c. At the edge of a cortico-hippocampal cell carpet, individual neurons and connections can be identified on top of electrodes and buried connection tracks alike. Between 1 Hz and 5 kHz, *polyMEA*s with PEDOT:PSS electrodes (Ø below 100 µm) had almost flat impedances of about 1.2 MΩ on average (Fig. 3d, blue dotted line). In contrast, gPDMS composite electrodes of same dimensions had significantly lower impedances of about 35 kΩ at 1 kHz with a logarithmic increase to about 15 MΩ at 1 Hz (Fig. 3d, black dashed line), which is typical for plain metal electrodes (Fig. 3d, orange line for Ø 30 µm TiN on Ti or on ITO electrodes). Despite their rather large electrode diameters and high impedances, PEDOT:PSS electrodes were able to capture action potentials and

local field fluctuations alike. And despite of the larger noise floor between ~ 20 µV (with gPDMS counter electrode or Pt wire GND) and 50 - 80 µV (with internal PEDOT:PSS counter electrode), signal-to-noise ratios (S/N) were typically 5 for neural recordings and up to 100 for cardiomyocyte recordings. This was confirmed with cortico-hippocampal co-cultures (Fig. 3f), retinal whole mounts and acute cardiac tissue preparations (both not shown). Local field responses to visual stimuli in epicortical recordings from the visual cortex of mice were clearly visible after 59x averaging (Fig. 3g).

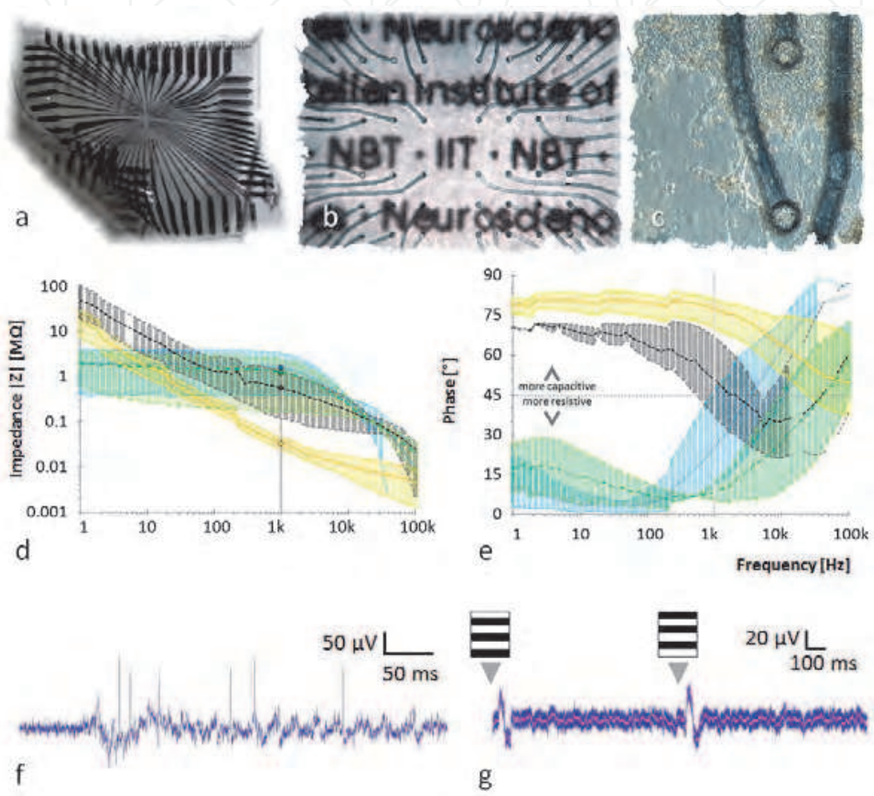

Fig. 3. **a**) *polyMEA* flexibility (~ 300 µm thick, with gPDMS composite conductor). **b**) Transparency of the PDMS substrate and of the PEDOT:PSS thin-film electrodes and buried tracks at the center of a *polyMEA* on top of a printout with letters of point 3 font size. **c**) Neurons of a cortico-hippocampal network (38 DIV) can be imaged and individually distinguished through the Ø 80 µm PEDOT:PSS electrodes and buried tracks. **d**) Impedance of Ø 80 µm PEDOT:PSS (blue) or gPDMS (black) electrodes, or of PEDOT:PSS electrodes with gPDMS pad fillings (green) compared to that of Ø 30 µm TiN-coated Ti or ITO electrodes of commercial MEAs (yellow). Dashed lines indicate averages, dotted borders extreme values. All spectra were recorded in saturated KCl. **e**) Phases for the electrode types and configurations mentioned in d). **f**) Simultaneous recording of action potentials on top of local field fluctuations from cortico-hippocampal co-cultures (rat E18, 38 DIV) on top of a PEDOT:PSS film electrode. **g**) Stimulus-induced local field potentials (after 59x averaging) captured by one out of 16 PEDOT:PSS film electrodes in epicortical recordings from the visual cortex of an anesthetized rat upon pattern reversal (arrows) of a grating as the visual cue. Blue trace: no filter; red trace: 200 Hz low pass filter. In both cases, a Pt wire served as a counter electrode. (Blau *et al.*, 2011).

Judging from the low phase of the impedance at low frequencies, the electrodes of the *polyMEA* devices show mostly resistive behavior. As discussed above, stimulation electrodes are usually designed to have a highly capacitive character (Cogan, 2008). Theoretically, the polymer electrodes therefore may need to be altered in postprocessing steps to increase their capacitance. However, impedance spectra were taken in a non-physiological scenario. Several groups have already demonstrated that PEDOT-decorated electrodes are good and sufficiently stable performers in neural stimulation experiments with a CSC of 2.3 - 15 mC/cm^2, which is already close to the 25 mC/cm^2 reported for IrO_x stimulation electrodes (Merrill *et al.*, 2005; Cui & Zhou, 2007; Cogan, 2008; Wilks *et al.*, 2009; Boretius *et al.*, 2011).
We tested 80 µm PEDOT:PSS and gPDMS electrodes on dense carpets of cortical and hippocampal neurons from rats in cultured neural networks for their suitability as voltage-controlled stimulation electrodes without success[24]. It may very well be that polymer electrodes of same or different diameters will nevertheless perform sufficiently well as stimulation electrodes when resorting to charge-controlled stimulation protocols or different stimulation waveforms. It is furthermore likely that, apart from the dimensional and electrical properties of an electrode and the medium composition, the distance and the capacitive and dielectric properties of the lipid double layer of the cell membrane have a larger than thought impact on the CSC[25]. If true, the stimulation performance of an electrode should depend on the type of cellular environment it is tested in.

1.3.6 Interconnection technologies

Connecting a microelectrode array to any kind of electronics is a critical issue. The mechanical clamping of contact pads requires a mechanism that is difficult to miniaturize and which might simply detach. Classical (wire) bonding introduces materials with limited flexibility that, due to stress and/or the contact chemistry between the different materials (including the humidity absorbed by a packaging compound), become the location of corrosion and break. By design, *polyMEA* arrays may alleviate the bonding issue. When the microchannel tracks are filled with elastomeric gPDMS (or alternatively with hydrogel conductors (Guiseppi-Elie, 2010)), they may be bent and twisted to a large degree. This property, together with the liberty to shape channels with increasing volumes downstream of the electrodes, allows for integrating ribbon cable-type wiring to external electronics as part of the electrode array. Thus, the point of connection may be placed wherever the mechanical stress onto the connector may be least. In one experimental approach, the gPDMS connection pads at the end of a supracortical prototype array were simply slipped into a standard dual row connector during their temporary depression (Fig. 4). Upon pressure release, the rubbery gPDMS was wedged by the pins, thus ensuring proper seating and electrical connectivity. And because the thickness of the back insulation layer of an *in vivo polyMEA* can be applied non-uniformly[26] (*e.g.*, thin at the recording site, thick at the

[24] Stimulation was based on charge-balanced biphasic voltage pulses not exceeding ±900 mV and 100 µs duration. Both polarity sequences (+, then -; -, then +) were tried.
[25] For a circular section of the cell membrane with a diameter matching that of commonly used electrodes (10 - 50 µm), the separated charge Q on the intracellular and extracellular side of the membrane during the resting (~ - 60 mV) or the action potential (~ 100 mV) is on the order of the CSC (several mC/cm^2) of above mentioned stimulation electrodes.
[26] Non-uniform, wedge-like shaping of a device only requires the covering of the non-cured PDMS backside insulation by a sheet positioned in a ramp-like configuration during its curing. For acute ramp angles, adhesion forces between the PDMS and the sheet will prevent PDMS efflux.

connector site), the contact pressure can be tuned to fit different connector types. The concept resembles that of zebra strip connectors. After insertion, probe and connector can be fixated by sewing and be encapsulated by PDMS or epoxies.

1.3.7 Shielding

Because long, and in particular, high-impedance wires may act like antennas which tend to pick up noise from the environment, they are usually avoided. Instead, high-to-low impedance conversion electronics are placed as closely to the electrodes as possible (as in 'active' MEA devices). However, today, the rigidity of any type of conversion electronics would still compromise device flexibility. Therefore, proper shielding (like in coaxial cables) remains the only alternative. Also in this case, PEDOT:PSS or gPDMS may substitute graphite-based conductive lacquers to create a mechanically more flexible, tightly device-wrapping shielding. When graphite is mixed into non-cured PDMS, the viscosity of the paste, once it has reached the desired conductivity, can be decreased temporarily with solvents such as iso-propanol. The external surface[27] of a device can thus be painted with such slurry gPDMS mix, which is then cured at elevated temperatures (80 °C – 150 °C). During the curing, the solvent will evaporate, resulting in a homogeneous conductive coating. It can be insulated by an upper coat of non-conductive PDMS. If a spot of the conductive gPDMS is kept deinsulated, it can serve as a counter electrode as part of the gPDMS shield. And, if necessary, the impedance of the gPDMS spot can be further tuned by electrochemical deposition of other conductors.

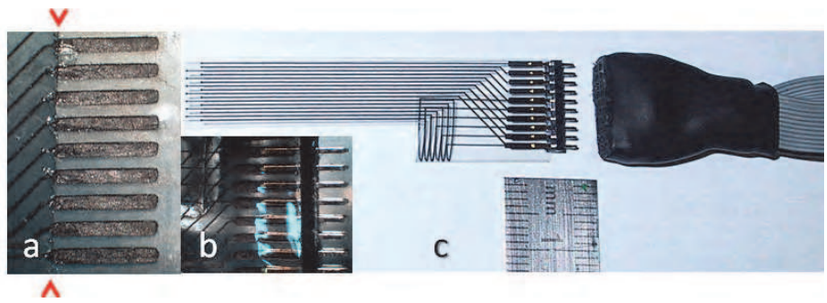

Fig. 4. **a**) gPDMS pads and tracks embedded in a 200 µm thick, still unfolded PDMS scaffold. Tracks had been topside-insulated by a thin film of PDMS. Pads (and electrodes, not shown) had been protected by scotch tape (red arrows indicate ridge after tape removal). **b**) Zoom onto pads slipped in between and squeezed by the pins of a standard 1.27 mm pitch, dual row, double pin connector, encapsulated by PDMS. **c**) Folded supracortical dummy probe demonstrating the slip-in concept. The flexibility of the PDMS scaffold and gPDMS tracks allows probe bending by 180° without compromising conductivity.

1.3.8 Other observations

For some not-yet understood and investigated reasons, PDMS seems to provide a more favorable surface for cell and tissue adhesion than other common culture substrates. In two acute slice experiments (retinal whole mounts) it was observed that, after an initial weigh-

[27] After a brief exposure of PDMS to oxygen plasma, PDMS can be permanently bonded to itself. In this case, a short oxygen-plasma treatment of the device will enhance the adhesion of the shielding layer to the PDMS surface. Such plasma exposure did not have any detrimental effect on PEDOT:PSS electrodes.

down by a nylon-stocking ensheathed platinum U-wire for enhancing the tissue electrode contact, the weight could be removed after 30 minutes without compromising the signal quality. While the PDMS and the electrodes had been coated with poly-D-lysine and laminin in a standard procedure for enhancing cell adhesion on MEAs, this type of stickiness had never been observed in our lab with insulation layers made of silicon nitride, silicon dioxide (glass) or polymer (photo-) resists such as SU-8 or polyimide. A similar observation has been reported by Guo *et al.* (Guo *et al.*, 2010). There, however, the improved contact to the tissue surface was mainly attributed to the geometries of the conical well encasing of the electrodes. At this point, it is not yet clear to what degree the short O_2 plasma hydrophilization[28] of the PDMS (for the better wetting with the adhesion mediators) contributed to its enhanced tissue interaction by not only altering the surface chemistry but also its morphology (Cvelbar *et al.*, 2003). A process-related micro- or nano-texturing of the PDMS surface may have played a role as well (Barr *et al.*, 2010). However, the most likely cause may be the tendency of silicones to absorb lipids (*e.g.*, from the cell membrane) resulting in partial cell or debris fusion with the PDMS surface and its dimensional swelling (Mchenry *et al.*, 1970; Colas & Curtis, 2004).
Preliminary results indicate that PEDOT:PSS can be embedded into a polymer matrix made of polyvinyl alcohol (PVA), glycerin and a di- or tricarboxylic acid as a crosslinker to render the PVA insoluble. However, this composite of high transparency and largely uncompromised conductivity will slightly swell in an aqueous environment. While a change in device geometries within the body is generally undesirable, a slight swelling of a polymer and/or its (hydrogel) electrodes may actually be favorable to enhance the electrode-tissue contact after device insertion. The water-uptake of PDMS itself is very low (below 1%). However, this might be just sufficient to stabilize device position within the tissue.

1.3.9 Open issues

As mentioned before, PDMS is very hydrophobic. Therefore, it is not wettable by aqueous or polar dispersions of organic conductors. Oxygen plasma treatment will render the PDMS surface hydrophilic by creating and exposing hydroxyl, carboxyl and peroxide groups on its surface, though. Depending on the storage conditions, this hydrophilicity is temporally more or less stable (Donzel *et al.*, 2001). Under ambient conditions, it will usually degrade rapidly after the first 30 minutes. It can be anticipated that with shrinking channel feature sizes, the presented method of filling these channels (by coating the entire scaffold backside with the CP dispersion and then scraping it from the plateaus after the partial evaporation of the solvent) may not necessarily work well anymore. However, by playing with the two extremes of wettability, a channel-only plasma treatment may solve the problem. By temporarily covering the *polyMEA* with two adhesive sheets on both sides during plasma exposure, only the channel walls will be hydrophilized. After sheet removal and upon spreading the dispersion onto the scaffold, it will self-distribute within the channels only. For each channel geometry, finding the proper plasma parameters (power, frequency, pressure, temperature, time) might not be trivial, though.
While the softness and flexibility of all-polymer MEAs is one of their main assets, they have one major drawback: a MEA will not be easy to insert into dense tissue. A removable insertion device may alleviate this problem, though. During device fabrication, stiffer insertion and guidance aids could be embedded into the polymer microchannel scaffold

[28] Plasma surface activation parameters for all types of MEAs stayed in the following ranges: One to three minutes at 30 – 60 W at 2.45 GHz in a 0.2 – 0.4 mbar pure oxygen atmosphere.

such as anti-stick-coated polymer or glass fibers, which would then be withdrawn once the *polyMEA* is in its final position.
The used type of PDMS already breaks after 100% tear. Softer and more stretchable polyurethanes or silicones are available that would render the devices even more flexible and tear-resistant. However, most of them have still to be tested for their biocompatibility. And some of them are only milky translucent, which make them less suitable for concurrent cell imaging studies.

1.3.10 Optional strategies and future directions

The flexibility of PDMS can be exploited for fabricating spherically bent neural probes that may become useful as retinal implants or for electroretinogram recordings as described *e.g.*, by Rodger *et al.* for parylene-based platinum electrode arrays (Rodger *et al.*, 2008). While the current master production gives microstructures on a plane, a copy thereof may take on any shape. It only requires the placing of a PDMS scaffold onto the inverted shape of the desired topography during master reproduction in epoxy. The bending of the PDMS slab will certainly distort some of the microchannel features. But as long as the curvatures are not too sharp, electrode geometries will not be compromised. The concept is sketched out in Fig. 5.

Fig. 5. Concept of fabricating non-planar *polyMEA*s. **a**) Replica-molding of a PDMS *polyMEA* microchannel scaffold (light blue) from planar master (orange). **b**) Fitting of the planar *polyMEA* scaffold into a non-planar template (black). **c**) Filling of shaped *polyMEA* microcavities with epoxy (green). **d**) After lifting off the template and removing the curved *polyMEA* from the cured epoxy, the non-planar epoxy master copy is coated with uncured PDMS and covered by the curved template. e) Removal of epoxy master copy and template after curing of PDMS gives a non-planar *polyMEA* microchannel scaffold.

Similar to classical soft-lithography, the microchannels could also serve for the assisted transfer of conductive patterns onto other carrier substrates (Fig. 6). When placed onto a (nano-porous) carrier (*e.g.*, a (filter) membrane) (Fig. 6-1), the channels may be filled with any kind of colloidal conductor material (Fig. 6-2). Upon applying a vacuum (underneath the membrane), the solvent will evaporate thereby leaving a conductor pattern on the membrane (Fig. 6-3). By filling the electrode and pad cavities with a sacrificial paste (*e.g.*, wax) (Fig. 6-4), removing the microchannel scaffold (Fig. 6-5), spin coating an insulation layer on the top (and bottom) side of the carrier (Fig. 6-6) and removing the sacrificial plugs from electrodes and pads in a final step (Fig. 6-7), a CP electrode array with design features similar to that reported by Guo *et al.* can be generated in the most straightforward and cost-efficient fashion (Guo *et al.*, 2010).
PEDOT:PSS can be purchased as an inkjet-compatible formulation. Thus, the filling of the microchannels with the conductor could not only be further automated, but different thicknesses or blends be deposited in different regions.
Alternatively, after the local laser-assisted alteration of the PDMS channel surfaces and the autocatalytic deposition of a Pt priming layer (Dupas-Bruzek, Drean, *et al.*, 2009), EDOT or

other precursors could be polymerized electrochemically to give electroconductive electrodes and tracks. The microchannels and the PDMS itself could be furthermore exploited in controlled drug-release strategies (Fig. 7b) (Colas, 2001; Musick *et al.*, 2009). Various neural implant design studies with included microfluidics have already been reported (*e.g.*, (Metz *et al.*, 2004; Suzuki *et al.*, 2004; Seidl & *Et al.*, 2010)) and their benefit been discussed recently (Musienko *et al.*, 2009). Although the stable coupling of the microchannels to outside fluidics might be possible (*e.g.*, by making use of multilayer bonding concepts (Zhang *et al.*, 2010) or reversible mechanical, pressure- or vacuum-assisted interconnection strategies (Chen & Pan, 2011)), without doubt it will be even more challenging than the design of fail-proof electrical connectors as discussed above.

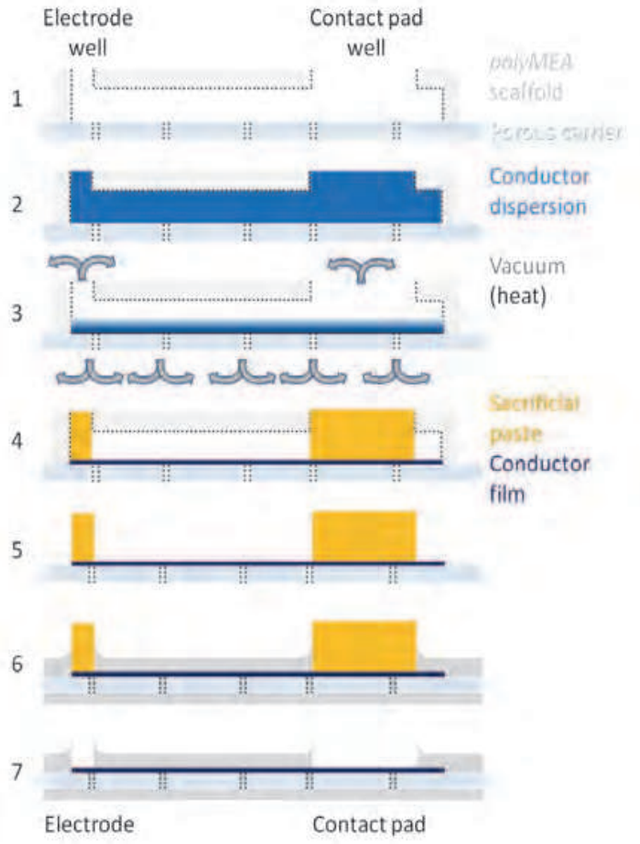

Fig. 6. *polyMEA* scaffold-assisted microelectrode patterning of thin-film carrier substrates. **1**) Placing of scaffold onto carrier and **2**) filling of microchannel cavities with conductor dispersion. **3**) Solvent evaporation leaves micropatterned conductor traces on the carrier. **4**) Temporary protection of electrodes and pads by application of a sacrificial paste through electrode and pad through-holes, **5**) removal of scaffold and **6**) application of top-side insulation layer (*e.g.*, by spin- or dip-coating) and **7**) removal of paste to deinsulate electrodes and pads.

With or without taking advantage of microfluidic connectors, neural processes could grow into the microchannels (Fig. 7b, left) as demonstrated by various groups (Morin *et al.*, 2005; Claverol-Tinture *et al.*, 2007; Benmerah *et al.*, 2009; Lacour *et al.*, 2010). This would increase the likelihood of identifying the actual origin of the bioelectrical signals. Alternatively, the

preloading of empty or CP-coated microchannels with slow-release (electroconductive) hydrogels carrying diverse drugs could be pursued (Fig. 7a), thereby steering neural differentiation, regeneration and activity with growth or signaling factors, alleviating probe insertion damage by antibiotics and anti-inflammatory drugs, or attenuating the formation of glial scars by mitotic inhibitors (Peppas *et al.*, 2006; Guiseppi-Elie, 2010). In that case, the electrical conductivity of the gel should be sufficiently high to warrant the coupling between the neuron and the conductive PEDOT:PSS film covering the microchannel walls. Alternatively or in combination, the PDMS itself could be loaded with drugs that are either soluble in PDMS or stored in porous cavities in a local silicone co-formulation. Delivering organic drugs through polymeric microchannels bears the risk of undesirable dissolution and accumulation of the compounds within the polymer over time, though. PDMS is particular prone to absorb *e.g.*, organic solvents (Lee *et al.*, 2003). In consequence, the absorption and release kinetics would have to be tested for each substance. While this absorption behavior could be a disadvantage in acute studies, it may become advantageous for chronic drug delivery where a slow and constant release of a drug is desired. In combination with the local deposition of photoelectric polymers, light-mediated electrical stimulation sites could be created (Fig. 7c) (Antognazza *et al.*, 2009; Facchetti, 2010; Ghezzi *et al.*, 2011). On a similar line, optical fibers or waveguides could be embedded into these channels for the light stimulation of optogenetic probes (Fig. 7d) (Im *et al.*, 2011). Neural activity from light-responsive neurons could thus be recorded from the PEDOT:PSS electrodes at the end of PEDOT:PSS-coated channels upon their optical stimulation through the very same channel.

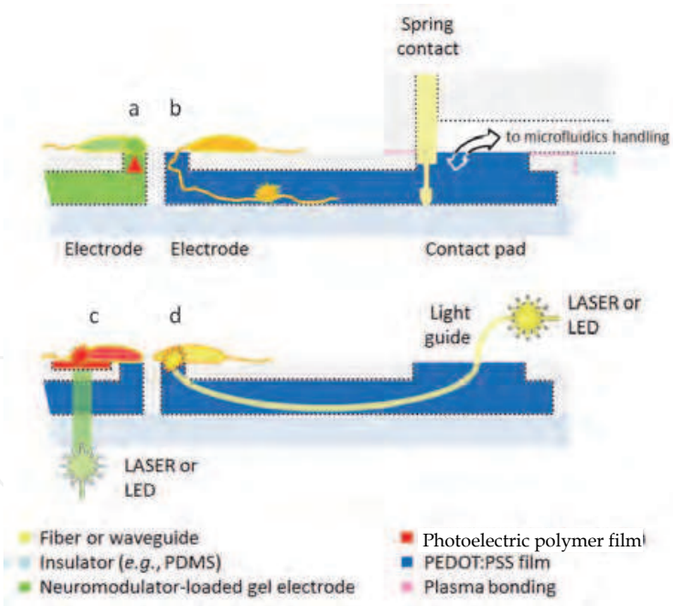

Fig. 7. Conceptual device enhancements. Delivering drugs **a**) passively through microchannel-embedded gel electrodes or **b**) actively by resorting to multilayer bonding concepts reported *e.g.* by Zhang *et al.* (Zhang *et al.*, 2010) or reversible mechanical, pressure- or vacuum-assisted interconnection strategies (*e.g.*, "fit-2-flow" (Chen & Pan, 2011)). Recording from neural processes after their ingrowth into PEDOT:PSS coated electrode microchannels. **c**) Photo stimulation of neurons through patterned photoelectric polymer films. **d**) Optical stimulation of optogenetically engineered neurons through channel-embedded waveguides or fiber optics.

2. Conclusions

Neuroprosthetic devices should mimic as best as possible the tissue they are placed into. The tissue would then accept them as its own or just ignore them. They should furthermore be chemically, mechanically and functionally time-invariant for uncompromised performance. Fabricating electrode arrays exclusively from soft polymeric materials may be one step into that direction. The innovative concept of filling bi- or multi-level microchannel electrode array scaffolds with polymer conductors opens several new routes for designing and fabricating neuroprosthetic devices not only on the laboratory bench, but also through existing replica mass production schemes (*e.g.*, mold-injection, hot-embossing). In contrast to metal MEAs (Sadleir *et al.*, 2005), polymer conductors may turn out to be compatible with computer tomography (CT) and magnetic resonance imaging (MRI), minimizing or avoiding image artifacts (Chen & Wiscombe, 1998; Flanders & Schwartz, 2008). Given the vast choice of insulation and conductor materials, device properties and performance can be tuned in a multitude of ways. While thin coatings of the microchannel walls with PEDOT:PSS lead to largely transparent devices suitable for combined electrophysiological and microscopy *in vitro* studies, currently, film stability with respect to bending and stretching is still limited. Nevertheless, depending on the fabrication approach, electrodes can be shaped as ring electrodes or classical area electrodes. Alternatively, channels can be filled entirely with rubber-like gPDMS or other conductive PDMS or PU composites, rendering the devices excellently stable to bending and stretching. If both transparency and flexibility are required, a hybrid strategy of combining PEDOT:PSS electrodes with gPDMS tracks and connector pads may be chosen. While the presented results refer to proof-of-concept studies with *polyMEA*s still having rather large electrode and track dimensions, there is no conceptual hurdle that prevents their further miniaturization. It can thus be foreseen that the presented *polyMEA* concept heralds a new generation of implantable neuroprosthetic electrode arrays.

3. Acknowledgements

Several talented students and researchers contributed to the development and evolution of the various *polyMEA* devices. Their enthusiasm, help and dedication is greatly appreciated. In particular, I would like to thank Angelika Murr, Sandra Wolff, Christian Dautermann, Stefan Trellenkamp, Jens Wüsten and Mario Cerino for their support in exploring diverse device designs including their fabrication and testing, Tanja Neumann, Simone Riedel, Marina Nanni, Francesca Succol, and Maria Teresa Tedesco for their assistance in cell culture preparation and maintenance, Evelyne Sernagor for the preparation of retinal whole mounts, Paolo Medini and Giuliano Iurilli for epicortical recordings, Laura Gasparini and Francesco Difato for support in microscopy, Giacomo Pruzzo for his advice and assistance in developing various electronic gadgets, Tommaso Fellin for insightful discussions on future *polyMEA* exploitation pathways, Christiane Ziegler for providing the startup infrastructure and research environment, Sergio Martinoia and the Dept. of Biophysical and Electronic Engineering at the University of Genoa for temporary lab access, and Fabio Benfenati for subsequent support in shaping the *polyMEA* research line. A generous PDMS sample provided by Wacker Chemie AG is highly appreciated. This work is supported by the Italian Institute of Technology Foundation.

4. References

Abidian, M.R., Corey, J.M., Kipke, D.R. & Martin, D.C. (2010). Conducting-polymer nanotubes improve electrical properties, mechanical adhesion, neural attachment, and neurite outgrowth of neural electrodes, *Small,* Vol. 6 No. 3, pp. 421-429.

Ahn, B.Y., Duoss, E.B., Motala, M.J., Guo, X., Park, S.I., Xiong, Y., Yoon, J., Nuzzo, R.G., Rogers, J.A. & Lewis, J.A. (2009). Omnidirectional printing of flexible, stretchable, and spanning silver microelectrodes, *Science,* Vol. 323 No. 5921, pp. 1590-1593.

Antognazza, M.R., Ghezzi, D., Musitelli, D., Garbugli, M. & Lanzani, G. (2009). A hybrid solid-liquid polymer photodiode for the bioenvironment, *Applied Physics Letters,* Vol. 94 No. 24, pp. 243501.

Asplund, M., Nyberg, T. & Inganas, O. (2010). Electroactive polymers for neural interfaces, *Polymer Chemistry,* Vol. 1 No. 9, pp. 1374-1391.

Ateh, D.D., Navsaria, H.A. & Vadgama, P. (2006). Polypyrrole-based conducting polymers and interactions with biological tissues, *J R Soc Interface,* Vol. 3 No. 11, pp. 741-752.

Barr, S., Hill, E. & Bayat, A. (2010). Patterning of novel breast implant surfaces by enhancing silicone biocompatibility, using biomimetic topographies, *Eplasty,* Vol. 10, pp. e31.

Baumann, W., Schreiber, E., Krause, G., Stüwe, S., Podssun, A., Homma, S., Anlauf, H., Freund, I. & Lehmann, M. (2002). Multiparametric neurosensor microchip, in *Eurosensors XVI* ISBN, Prag, pp. 1169-1172

Baumann, W.H., Lehmann, M., Schwinde, A., Ehret, R., Brischwein, M. & Wolf, B. (1999). Microelectronic sensor system for microphysiological application on living cells, *Sensors and Actuators B: Chemical,* Vol. 55 No. 1, pp. 77-89.

Bear, M.F., Connors, B.W. & Paradiso, M.A. (2007). *Neuroscience: Exploring the brain*, Lippincott Williams & Wilkins, Baltimore.

Beattie, A.J., Curtis, A.S.G., Wilkinson, C.D.W. & Riehle, M. (2009). Nanomaterials for neural interfaces: Emerging new function and potential applications, in Offenhäusser, A. & Rinaldi, R. (Eds.), *Nanobioelectronics - for electronics, biology, and medicine*. Springer New York, 978-0-387-09459-5, pp. 277-286.

Benmerah, S., Lacour, S.P. & Tarte, E. (2009). Design and fabrication of neural implant with thick microchannels based on flexible polymeric materials, *Conference Proceedings, Annual International Conference of the IEEE Engineering in Medicine and Biology Society,* Vol. 2009, pp. 6400-6403.

Berdondini, L., Chippalone, M., Van Der Wal, P.D., Imfeld, K., De Rooij, N.F., Koudelka-Hep, M., Tedesco, M., Martinoia, S., Van Pelt, J., Le Masson, G. & Garenne, A. (2006). A microelectrode array (mea) integrated with clustering structures for investigating in vitro neurodynamics in confined interconnected sub-populations of neurons, *Sensors and Actuators B,* Vol. 114, pp. 530-541.

Berdondini, L., Imfeld, K., Maccione, A., Tedesco, M., Neukom, S., Koudelka-Hep, M. & Martinoia, S. (2009). Active pixel sensor array for high spatio-temporal resolution electrophysiological recordings from single cell to large scale neuronal networks, *Lab on a Chip,* Vol. 9 No. 18, pp. 2644-2651.

Berdondini, L., Massobrio, P., Chiappalone, M., Tedesco, M., Imfeld, K., Maccione, A., Gandolfo, M., Koudelka-Hep, M. & Martinoia, S. (2009). Extracellular recordings from locally dense microelectrode arrays coupled to dissociated cortical cultures, *J Neurosci Methods,* Vol. 177 No. 2, pp. 386-396.

Blau, A., Murr, A., Wolff, S., Sernagor, E., Medini, P., Iurilli, G., Ziegler, C. & Benfenati, F. (2011). Flexible, all-polymer microelectrode arrays for the capture of cardiac and neuronal signals, *Biomaterials,* Vol. 32 No. 7, pp. 1778-1786.

Bongard, M., Gabriel, G., Villa, R., Gomez, R., Benito, N. & Fernandez, E. (2010). Spike recordings from ganglion cell populations using a new type of carbon nanotubes surface multielectrodes, in Stett, A. (Ed.), *Proceedings of the 7th Int. Meeting on Substrate-Integrated Microelectrode Arrays, June 29 – July 2*. BIOPRO Baden-Württemberg GmbH, ISBN, Reutlingen, pp. 259-260.

Bonifazi, P. & Fromherz, P. (2002). Silicon chip for electronic communication between nerve cells by non-invasive interfacing and analog–digital processing, *Advanced Materials,* Vol. 14 No. 17, pp. 1190-1193.

Boppart, S.A., Wheeler, B.C. & Wallace, C.S. (1992). A flexible perforated microelectrode array for extended neural recordings, *IEEE Transactions on Biomedical Engineering,* Vol. 39 No. 1, pp. 37-42.

Boretius, T., Schuettler, M. & Stieglitz, T. (2011). On the stability of poly-ethylenedioxythiopene as coating material for active neural implants, *Artificial Organs,* Vol. 35 No. 3, pp. 245-248.

Breckenridge, L.J., Wilson, R.J., Connolly, P., Curtis, A.S., Dow, J.A., Blackshaw, S.E. & Wilkinson, C.D. (1995). Advantages of using microfabricated extracellular electrodes for in vitro neuronal recording, *Journal of Neuroscience Research,* Vol. 42 No. 2, pp. 266-276.

Briquet, F., Colas, A. & Thomas, X. (1996). Silicones for medical use, in, ISBN, pp. 10.

Bucher, V., Brunner, B., Leibrock, C., Schubert, M. & Nisch, W. (2001). Electrical properties of a light-addressable microelectrode chip with high electrode density for extracellular stimulation and recording of excitable cells, *Biosensors & Bioelectronics,* Vol. 16 No. 3, pp. 205-210.

Butt, H.-J., Graf, K. & Kappl, M. (2003). *Physics and chemistry of interfaces*, Wiley, 3-527-40413-9, Weinheim.

Calixto, C.M.F., Mendes, R.K., Oliveira, A.C.D., Ramos, L.A., Cervini, P. & Cavalheiro, É.T.G. (2007). Development of graphite-polymer composites as electrode materials, *Materials Research,* Vol. 10, pp. 109-114.

Chen, A. & Pan, T. (2011). Fit-to-flow (f2f) interconnects: Universal reversible adhesive-free microfluidic adaptors for lab-on-a-chip systems, *Lab on a Chip,* Vol. 11 No. 4, pp. 727-732.

Chen, C. & Folch, A. (2006). A high-performance elastomeric patch clamp chip, *Lab on a Chip,* Vol. 6 No. 10, pp. 1338-1345.

Chen, J.C. & Wiscombe, B. (1998). Method and pdt probe for minimizing ct and mri image artifacts, in. Light Sciences Limited Partnership (Issaquah, WA), ISBN, pp. 15.

Cheung, K.C. (2007). Implantable microscale neural interfaces, *Biomed Microdevices,* Vol. 9 No. 6, pp. 923-938.

Clark, J.W. (1998). The origin of biopotentials, in Webster, J.G. (Ed.), *Medical instrumentation: Application and design* John Wiley and Sons, Inc., NY, pp. 121-182.

Claverol-Tinture, E., Cabestany, J. & Rosell, X. (2007). Multisite recording of extracellular potentials produced by microchannel-confined neurons in-vitro, *IEEE Transactions on Bio-medical Engineering,* Vol. 54 No. 2, pp. 331-335.

Cogan, S.F. (2008). Neural stimulation and recording electrodes, *Annual Review of Biomedical Engineering,* Vol. 10, pp. 275-309.

Colas, A. (2001). Silicones in pharmaceutical applications, in, ISBN, pp. 24.

Colas, A. & Curtis, J. (2004). Silicone biomaterials: History and chemistry, in Ratner, B.D., Hoffman, A.S., Schoen, F.J. & Lemans, J.E. (Eds.), *Biomaterials science - an introduction to materials in medicine*. Academic Press, 978-0-12-582463-7, pp. 80-86.

Collazos-Castro, J.E., Polo, J.L., Hernandez-Labrado, G.R., Padial-Canete, V. & Garcia-Rama, C. (2010). Bioelectrochemical control of neural cell development on conducting polymers, *Biomaterials,* Vol. 31 No. 35, pp. 9244-9255.

Connolly, P., Clark, P., Curtis, A.S.G., Dow, J.a.T. & Wilkinson, C.D. (1990). An extracellular microelectrode array for monitoring electrogenic cells in culture, *Biosensors & Biolelectronics,* Vol. 5, pp. 223-234.

Cui, X., Lee, V.A., Raphael, Y., Wiler, J.A., Hetke, J.F., Anderson, D.J. & Martin, D.C. (2001). Surface modification of neural recording electrodes with conducting polymer/biomolecule blends, *Journal of Biomedical Materials Research,* Vol. 56 No. 2, pp. 261-272.

Cui, X.T. & Zhou, D.D. (2007). Poly (3,4-ethylenedioxythiophene) for chronic neural stimulation, *Neural Systems and Rehabilitation Engineering, IEEE Transactions on,* Vol. 15 No. 4, pp. 502-508.

Cunningham, W., Mathieson, K., Mcewan, F.A., Blue, A., Mcgeachy, R., Mcleod, J.A., Morris-Ellis, C., O'shea, V., Smith, K.M., Litke, A. & Rahman, M. (2001). Fabrication of microelectrode arrays for neural measurements from retinal tissue, *Journal of Physics D: Applied Physics* No. 18, pp. 2804.

Curtis, J. & Colas, A. (2004). Medical applications of silicones, in Ratner, B.D., Hoffman, A.S., Schoen, F.J. & Lemans, J.E. (Eds.), *Biomaterials science - an introduction to materials in medicine*. Academic Press, 978-0-12-582463-7, pp. 697-707.

Cvelbar, U., Pejovnik, S., Mozetiè, M. & Zalar, A. (2003). Increased surface roughness by oxygen plasma treatment of graphite/polymer composite, *Applied Surface Science,* Vol. 210 No. 3-4, pp. 255-261.

Debusschere, B.D. & Kovacs, G.T.A. (2001). Portable cell-based biosensor system using integrated cmos cell-cartridges, *Biosensors and Bioelectronics,* Vol. 16 No. 7-8, pp. 543-556.

Difato, F., Maschio, M.D., Marconi, E., Ronzitti, G., Maccione, A., Fellin, T., Berdondini, L., Chieregatti, E., Benfenati, F. & Blau, A. (2011). Combined optical tweezers and laser dissector for controlled ablation of functional connections in neural networks, *Journal of Biomedical Optics,* Vol. 16 No. 5, pp. 051306-051309

Donzel, C., Geissler, M., Bernard, A., Wolf, H., Michel, B., Hilborn, J. & Delamarche, E. (2001). Hydrophilic poly(dimethylsiloxane) stamps for microcontact printing, *Advanced Materials,* Vol. 13 No. 15, pp. 1164-1167.

Dowling, J. (2008). Current and future prospects for optoelectronic retinal prostheses, *Eye,* Vol. 23 No. 10, pp. 1999-2005.

Dupas-Bruzek, C., Drean, P. & Derozier, D. (2009). Pt metallization of laser transformed medical grade silicone rubber: Last step toward a miniaturized nerve electrode fabrication process, *Journal of Applied Physics,* Vol. 106 No. 7, pp. 074913:074911-074915.

Dupas-Bruzek, C., Robbe, O., Addad, A., Turrell, S. & Derozier, D. (2009). Transformation of medical grade silicone rubber under nd:Yag and excimer laser irradiation: First step towards a new miniaturized nerve electrode fabrication process, *Applied Surface Science,* Vol. 255 No. 21, pp. 8715-8721.

Duport, S., Millerin, C., Muller, D. & Correges, P. (1999). A metallic multisite recording system designed for continuous long-term monitoring of electrophysiological activity in slice cultures, *Biosensors & Bioelectronics,* Vol. 14 No. 4, pp. 369-376.

Ehret, R., Baumann, W., Brischwein, M., Lehmann, M., Henning, T., Freund, I., Drechsler, S., Friedrich, U., Hubert, M.L., Motrescu, E., Kob, A., Palzer, H., Grothe, H. & Wolf, B. (2001). Multiparametric microsensor chips for screening applications, *Fresenius' Journal of Analytical Chemistry,* Vol. 369 No. 1, pp. 30-35.

Eick, S., Wallys, J., Hofmann, B., Van Ooyen, A., Schnakenberg, U., Ingebrandt, S. & Offenhäusser, A. (2009). Iridium oxide microelectrode arrays for in vitro stimulation of individual rat neurons from dissociated cultures, *Frontiers in Neuroengineering,* Vol. 2 No. 16, pp. 1-12.

Eschermann, J.F., Stockmann, R., Hueske, M., Vu, X.T., Ingebrandt, S. & Offenhausser, A. (2009). Action potentials of hl-1 cells recorded with silicon nanowire transistors, *Applied Physics Letters,* Vol. 95 No. 8, pp. 083703-083703.

Facchetti, A. (2010). Π-conjugated polymers for organic electronics and photovoltaic cell applications†, *Chemistry of Materials,* Vol. 23 No. 3, pp. 733-758.

Fejtl, M., Stett, A., Nisch, W., Boven, K.-H. & Möller, A. (2006). On micro-eletrode array revival: Its development, sophistication of recording and stimulation, in Taketani, M. & Baudry, M. (Eds.), *Advances in network electrophysiology. Using multi-electrode arrays.* Springer, 978-0-387-25857-7 (Print) 978-0-387-25858-4 (Online), New York, pp. 24-37.

Flanders, A., E. & Schwartz, E.D. (2008). Spinal trauma, in Atlas, S.W. (Ed.), *Magnetic resonance imaging of the brain and spine*. Wolters Kluwer Health, pp. 1564-1623.

Frey, U., Sedivy, J., Heer, F., Pedron, R., Ballini, M., Mueller, J., Bakkum, D., Hafizovic, S., Faraci, F.D., Greve, F., Kirstein, K.U. & Hierlemann, A. (2010). Switch-matrix-based high-density microelectrode array in cmos technology, *Solid-State Circuits, IEEE Journal of,* Vol. 45 No. 2, pp. 467-482.

Fromherz, P. (2006). Three levels of neuroelectronic interfacing, *Annals of the New York Academy of Sciences,* Vol. 1093 No. 1, pp. 143-160.

Fromherz, P., Offenhausser, A., Vetter, T. & Weiss, J.A. (1991). Neuron-silicon junction: A retzius cell of the leech on an insulated-gate field-effect transistor, *Science,* Vol. 252, pp. 1290-1293.

Gabriel, G., Gómez, R., Bongard, M., Benito, N., Fernández, E. & Villa, R. (2009). Easily made single-walled carbon nanotube surface microelectrodes for neuronal applications, *Biosensors and Bioelectronics,* Vol. 24 No. 7, pp. 1942-1948.

George, P.M., Lyckman, A.W., Lavan, D.A., Hegde, A., Leung, Y., Avasare, R., Testa, C., Alexander, P.M., Langer, R. & Sur, M. (2005). Fabrication and biocompatibility of polypyrrole implants suitable for neural prosthetics, *Biomaterials,* Vol. 26 No. 17, pp. 3511-3519.

Ghezzi, D., Antognazza, M.R., Dal Maschio, M., Lanzarini, E., Benfenati, F. & Lanzani, G. (2011). A hybrid bioorganic interface for neuronal photoactivation, *Nat Commun,* Vol. 2, pp. 166.

Gholmieh, G., Soussou, W., Han, M., Ahuja, A., Hsiao, M.C., Song, D., Tanguay, A.R., Jr. & Berger, T.W. (2006). Custom-designed high-density conformal planar multielectrode arrays for brain slice electrophysiology, *Journal of Neuroscience Methods,* Vol. 152 No. 1-2, pp. 116-129.

Giovangrandi, L., Gilchrist, K.H., Whittington, R.H. & T.A. Kovacs, G. (2006). Low-cost microelectrode array with integrated heater for extracellular recording of cardiomyocyte cultures using commercial flexible printed circuit technology, *Sensors and Actuators B: Chemical,* Vol. 113 No. 1, pp. 545-554.

Gong, X. & Wen, W. (2009). Polydimethylsiloxane-based conducting composites and their applications in microfluidic chip fabrication, *Biomicrofluidics,* Vol. 3 No. 1, pp. 12007.

Graimann, B., Allison, B. & Pfurtscheller, G. (2010). Brain-computer interfaces, in. Springer, ISBN, Berlin, pp. 300.

Green, R.A., Lovell, N.H. & Poole-Warren, L.A. (2010). Impact of co-incorporating laminin peptide dopants and neurotrophic growth factors on conducting polymer properties, *Acta Biomaterialia,* Vol. 6 No. 1, pp. 63-71.

Gross, G.W., Harsch, A., Rhoades, B.K. & Gopel, W. (1997). Odor, drug and toxin analysis with neuronal networks in vitro: Extracellular array recording of network responses, *Biosensors & Bioelectronics,* Vol. 12 No. 5, pp. 373-393.

Gross, G.W., Rieske, E., Kreutzberg, G.W. & Meyer, A. (1977). A new fixed-array multimicroelectrode system designed for long-term monitoring of extracellular single unit neuronal activity in vitro, *Neuroscience Letters* No. 6, pp. 101-105.

Gross, G.W., Wen, W.Y. & Lin, J.W. (1985). Transparent indium-tin oxide electrode patterns for extracellular, multisite recording in neuronal cultures, *Journal of Neuroscience Methods,* Vol. 15 No. 3, pp. 243-252.

Guimard, N.K., Gomez, N. & Schmidt, C.E. (2007). Conducting polymers in biomedical engineering, *Progress in Polymer Science,* Vol. 32 No. 8-9, pp. 876-921.

Guiseppi-Elie, A. (2010). Electroconductive hydrogels: Synthesis, characterization and biomedical applications, *Biomaterials,* Vol. 31 No. 10, pp. 2701-2716.

Gunning, D.E., Hottowy, P., Dabrowski, W., Hobbs, J.P., Beggs, J.M., Sher, A., Litke, A.M., Kenney, C.J. & Mathieson, K. (2010). High-density micro-needles for in vitro

neural studies, in Stett, A. (Ed.), *Proceedings of the 7th Int. Meeting on Substrate-Integrated Microelectrode Arrays, June 29 – July 2*. BIOPRO Baden-Württemberg GmbH, ISBN, Reutlingen, pp. 275-275.

Guo, L., Meacham, K.W., Hochman, S. & Deweerth, S.P. (2010). A pdms-based conical-well microelectrode array for surface stimulation and recording of neural tissues, *IEEE Transactions on Bio-medical Engineering,* Vol. 57 No. 10, pp. 2485-2494.

Haemmerle, H., Egert, U., Mohr, A. & Nisch, W. (1994). Extracellular recording in neuronal networks with substrate integrated microelectrode arrays, *Biosensors & Biolelectronics,* Vol. 9 No. 9-10, pp. 691-696.

Hai, A., Dormann, A., Shappir, J., Yitzchaik, S., Bartic, C., Borghs, G., Langedijk, J.P.M. & Spira, M.E. (2009). Spine-shaped gold protrusions improve the adherence and electrical coupling of neurons with the surface of micro-electronic devices, *Journal of the Royal Society Interface,* Vol. 6 No. 41, pp. 1153-1165.

Hai, A., Shappir, J. & Spira, M.E. (2010). In-cell recordings by extracellular microelectrodes, *Nat Meth,* Vol. 7 No. 3, pp. 200-202.

Hajjhassan, M., Chodavarapu, V. & Musallam, S. (2008). Neuromems: Neural probe microtechnologies, *Sensors,* Vol. 8 No. 10, pp. 6704-6726.

Hassler, C., Boretius, T. & Stieglitz, T. (2011). Polymers for neural implants, *Journal of Polymer Science Part B: Polymer Physics,* Vol. 49 No. 1, pp. 18-33.

Heer, F., Hafizovic, S., Ugniwenko, T., Frey, U., Franks, W., Perriard, E., Perriard, J.C., Blau, A., Ziegler, C. & Hierlemann, A. (2007). Single-chip microelectronic system to interface with living cells, *Biosensors & Bioelectronics,* Vol. 22 No. 11, pp. 2546-2553.

Held, J., Gaspar, J., Koester, P.J., Tautorat, C., Cismak, A., Heilmann, A., Baumann, W., Trautmann, A., Ruther, P. & Paul, O. (2008). Microneedle arrays for intracellular recording applications, in *Micro Electro Mechanical Systems, 2008. MEMS 2008. IEEE 21st International Conference on*, ISBN, pp. 268-271.

Held, J., Gaspar, J., Ruther, P., Hagner, M., Cismak, A., Heilmann, A. & Paul, O. (2010). Solid silver microneedle electrode arrays for intracellular recording applications, in Stett, A. (Ed.), *Proceedings of the 7th Int. Meeting on Substrate-Integrated Microelectrode Arrays, June 29 – July 2*. BIOPRO Baden-Württemberg GmbH, ISBN, Reutlingen, pp. 247-248.

Held, J., Heynen, J., Stumpf, A., Nisch, W., Burkhardt, C. & Stett, A. (2010). Micro pillar electrodes on meas for tissue stimulation, in Stett, A. (Ed.), *Proceedings of the 7th Int. Meeting on Substrate-Integrated Microelectrode Arrays, June 29 – July 2*. BIOPRO Baden-Württemberg GmbH, ISBN, Reutlingen, pp. 241-242.

Henle, C., Raab, M., Cordeiro, J., Doostkam, S., Schulze-Bonhage, A., Stieglitz, T. & Rickert, J. (2011). First long term in vivo study on subdurally implanted micro-ecog electrodes, manufactured with a novel laser technology, *Biomedical Microdevices,* Vol. 13 No. 1, pp. 59-68.

Hetke, J. & Anderson, D. (2002). Silicon microelectrodes for extracellular recording, in *Handbook of neuroprosthetic methods*. CRC Press, 978-0-8493-1100-0, pp. 29.

Heuschkel, M.O., Fejtl, M., Raggenbass, M., Bertrand, D. & Renaud, P. (2002). A three-dimensional multi-electrode array for multi-site stimulation and recording in acute brain slices, *J Neurosci Methods,* Vol. 114 No. 2, pp. 135-148.

Heuschkel, M.O., Wirth, C., Steidl, E.-M. & Buisson, B. (2006). Development of 3d multi electrode arrays for use with acute tussue slices, in Taketani, M. & Baudry, M. (Eds.), *Advances in network electrophysiology. Using multi-electrode arrays.* Springer, 978-0-387-25857-7 (Print) 978-0-387-25858-4 (Online), New York, pp. 69-111.

Hierlemann, A., Frey, U., Hafizovic, S. & Heer, F. (2011). Growing cells atop microelectronic chips: Interfacing electrogenic cells in vitro with cmos-based microelectrode arrays, *Proceedings of the IEEE,* Vol. 99 No. 2, pp. 252-284.

Hofmann, B., Katelhon, E., Schottdorf, M., Offenhausser, A. & Wolfrum, B. (2011). Nanocavity electrode array for recording from electrogenic cells, *Lab on a Chip*.

Hu, Z., Zhou, D.M., Greenberg, R. & Thundat, T. (2006). Nanopowder molding method for creating implantable high-aspect-ratio electrodes on thin flexible substrates, *Biomaterials,* Vol. 27 No. 9, pp. 2009-2017.

Huang, J.-R., Lin, W.-T., Huang, R., Lin, C.-Y. & Wu, J.-K. (2011). Conductive coating method to inhibit marine biofouling, in, ISBN.

Hutzler, M., Lambacher, A., Eversmann, B., Jenkner, M., Thewes, R. & Fromherz, P. (2006). High-resolution multi-transistor array recording of electrical field potentials in cultured brain slices, *Journal of Neurophysiology,* Vol. 96, pp. 1638--1645.

Im, M., Cho, I.-J., Wu, F., Wise, K.D. & Yoon, E. (2011). Neural probes integrated with optical mixer/splitter waveguides and multiple stimulation sites, in *24th IEEE International Conference on Micro Electro Mechanical Systems (MEMS)*, ISBN, Cancun, Mexico, pp. 1051-1054.

Imfeld, K., Garenne, A., Neukom, S., Maccione, A., Martinoia, S., Koudelka-Hep, M. & Berdondini, L. (2007). High-resolution mea platform for in-vitro electrogenic cell networks imaging, in *Engineering in Medicine and Biology Society, 2007. EMBS 2007. 29th Annual International Conference of the IEEE*, ISBN, pp. 6085-6088.

Inganäs, O. (2010). Hybrid electronics and electrochemistry with conjugated polymers, *Chemical Society Reviews,* Vol. 39 No. 7, pp. 2633-2642.

Israel, D.A., Barry, W.H., Edell, D.J. & Mark, R.G. (1984). An array of microelectrodes to stimulate and record from cardiac cells in culture, *American Journal of Physiology - Heart and Circulatory Physiology,* Vol. 247 No. 4, pp. H669-H674.

Jaber, F.T., Labeed, F.H. & Hughes, M.P. (2009). Action potential recording from dielectrophoretically positioned neurons inside micro-wells of a planar microelectrode array, *Journal of Neuroscience Methods,* Vol. 182 No. 2, pp. 225-235.

James, C.D., Spence, A.J., Dowell-Mesfin, N.M., Hussain, R.J., Smith, K.L., Craighead, H.G., Isaacson, M.S., Shain, W. & Turner, J.N. (2004). Extracellular recordings from patterned neuronal networks using planar microelectrode arrays, *IEEE Trans Biomed Eng,* Vol. 51 No. 9, pp. 1640-1648.

Janata, J. & Josowicz, M. (2003). Conducting polymers in electronic chemical sensors, *Nat Mater,* Vol. 2 No. 1, pp. 19-24.

Janders, M., Egert, U., Stelzle, M. & Nisch, W. (1996). Novel thin film titanium nitride micro-electrodes with excellent charge transfer capability for cell stimulation and sensing applications, in Boom, H., Robinson, C., Rutten, W., Neuman, M. & Wijkstra, H. (Eds.), *Proceedings of 18th Annual International Conference of the IEEE Engineering in Medicine and Biology Society*. Naturwissenschaftliches und Med. Inst. Reutlingen Germany

Jansen, H., Gardeniers, H., Boer, M.D., Elwenspoek, M. & Fluitman, J. (1996). A survey on the reactive ion etching of silicon in microtechnology, *Journal of Micromechanics and Microengineering,* Vol. 6 No. 1, pp. 14.

Proceedings of the 18th Annual International Conference of the IEEE Engineering in Medicine and Biology Society. `Bridging Disciplines for Biomedicine' (Cat. No.96CH36036). IEEE New York NY USA, ISBN, Amsterdam, Netherlands, pp. 245-247.

Jochum, T., Denison, T. & Wolf, P. (2009). Integrated circuit amplifiers for multi-electrode intracortical recording, *Journal of Neural Engineering,* Vol. 6 No. 1, pp. 012001.

Johnstone, A.F., Gross, G.W., Weiss, D.G., Schroeder, O.H., Gramowski, A. & Shafer, T.J. (2010). Microelectrode arrays: A physiologically based neurotoxicity testing platform for the 21st century, *Neurotoxicology,* Vol. 31 No. 4, pp. 331-350.

Jung, S., Kang, C., Jung, I., Lee, S., Jung, P. & Ko, J. (2008). Fabrication of curved copper micromesh sheets using flexible pdms molds, *Microsystem Technologies,* Vol. 14 No. 6, pp. 829-833.

Kahol, P.K., Ho, J.C., Chen, Y.Y., Wang, C.R., Neeleshwar, S., Tsai, C.B. & Wessling, B. (2005). On metallic characteristics in some conducting polymers, *Synthetic Metals,* Vol. 151 No. 1, pp. 65-72.

Kawana, A. & Jimbo, Y. (1999). Neurointerface: Interfaces of neuronal networks to electrical circuit, in *Micro Electro Mechanical Systems, 1999. MEMS '99. Twelfth IEEE International Conference on*, ISBN, pp. 14-20.

Keefer, E.W., Botterman, B.R., Romero, M.I., Rossi, A.F. & Gross, G.W. (2008). Carbon nanotube coating improves neuronal recordings, *Nat Nano,* Vol. 3 No. 7, pp. 434-439.

Kirkpatrick, S. (1973). Percolation and conduction, *Reviews of Modern Physics,* Vol. 45 No. 4, pp. 574.

Klemic, K.G., Klemic, J.F. & Sigworth, F.J. (2005). An air-molding technique for fabricating pdms planar patch-clamp electrodes, *Pflügers Archiv European Journal of Physiology,* Vol. 449 No. 6, pp. 564-572.

Koester, P.J., Buehler, S.M., Stubbe, M., Tautorat, C., Niendorf, M., Baumann, W. & Gimsa, J. (2010). Modular glass chip system measuring the electric activity and adhesion of neuronal cells-application and drug testing with sodium valproic acid, *Lab on a Chip,* Vol. 10 No. 12, pp. 1579-1586.

Kotov, N.A., Winter, J.O., Clements, I.P., Jan, E., Timko, B.P., Campidelli, S., Pathak, S., Mazzatenta, A., Lieber, C.M., Prato, M., Bellamkonda, R.V., Silva, G.A., Kam, N.W.S., Patolsky, F. & Ballerini, L. (2009). Nanomaterials for neural interfaces, *Advanced Materials,* Vol. 21 No. 40, pp. 3970-4004.

Lacour, S., Benmerah, S., Tarte, E., Fitzgerald, J., Serra, J., Mcmahon, S., Fawcett, J., Graudejus, O., Yu, Z. & Morrison, B. (2010). Flexible and stretchable micro-electrodes for in vitro and in vivo neural interfaces, *Medical and Biological Engineering and Computing,* Vol. 48 No. 10, pp. 945-954.

Lambacher, A., Vitzthum, V., Zeitler, R., Eickenscheidt, M., Eversmann, B., Thewes, R. & Fromherz, P. (2011). Identifying firing mammalian neurons in networks with high-resolution multi-transistor array (mta), *Applied Physics A: Materials Science & Processing,* Vol. 102 No. 1, pp. 1-11.

Lange, U., Roznyatovskaya, N.V. & Mirsky, V.M. (2008). Conducting polymers in chemical sensors and arrays, *Analytica Chimica Acta,* Vol. 614 No. 1, pp. 1-26.

Lapitska, N., Gosseries, O., Delvaux, V., Overgaard, M., Nielsen, F., Maertens De Noordhout, A., Moonen, G. & Laureys, S. (2009). Transcranial magnetic stimulation in disorders of consciousness, *Rev Neurosci,* Vol. 20 No. 3-4, pp. 235-250.

Larmagnac, A., Musienko, P., Vörös, J. & Courtine, G. (2010). Highly stretchable pdms-based multi-electrode array for epidural electrical stimulation to regain motor function after spinal cord injury, in Stett, A. (Ed.), *Proceedings of the 7th Int. Meeting on Substrate-Integrated Microelectrode Arrays, June 29 – July 2*. BIOPRO Baden-Württemberg GmbH, ISBN, Reutlingen, pp. 229-230.

Leach, J.B., Achyuta, A.K. & Murthy, S.K. (2010). Bridging the divide between neuroprosthetic design, tissue engineering and neurobiology, *Front Neuroengineering,* Vol. 2, pp. 18.

Lebedev, M.A., Crist, R.E. & Nicolelis, M.a.L. (2008). Building brain-machine interfaces to restore neurological functions, in Nicolelis, M.A.L. (Ed.), *Methods for neural ensemble recordings*. CRC Press, Boca Raton.

Lee, J.N., Park, C. & Whitesides, G.M. (2003). Solvent compatibility of poly(dimethylsiloxane)-based microfluidic devices, *Analytical Chemistry,* Vol. 75 No. 23, pp. 6544-6554.

Li, L. & Fourkas, J.T. (2007). Multiphoton polymerization, *Materials Today,* Vol. 10 No. 6, pp. 30-37.

Logan, B.E. (2009). Exoelectrogenic bacteria that power microbial fuel cells, *Nat Rev Microbiol,* Vol. 7 No. 5, pp. 375-381.

Ludwig, K.A., Langhals, N.B., Joseph, M.D., Richardson-Burns, S.M., Hendricks, J.L. & Kipke, D.R. (2011). Poly(3,4-ethylenedioxythiophene) (pedot) polymer coatings facilitate smaller neural recording electrodes, *Journal of Neural Engineering,* Vol. 8 No. 1, pp. 014001.

Malarkey, E.B. & Parpura, V. (2010). Carbon nanotubes in neuroscience, *Acta Neurochir Suppl,* Vol. 106, pp. 337-341.

Marin, C. & Fernandez, E. (2010). Biocompatibility of intracortical microelectrodes: Current status and future prospects, *Frontiers in Neuroengineering,* Vol. 3 No. 8, pp. 5.

Mathieson, K., Kachiguine, S., Adams, C., Cunningham, W., Gunning, D., O'shea, V., Smith, K.M., Chichilnisky, E.J., Litke, A.M., Sher, A. & Rahman, M. (2004). Large-

area microelectrode arrays for recording of neural signals, *Nuclear Science, IEEE Transactions on,* Vol. 51 No. 5, pp. 2027-2031.

Mchenry, M., Smeloff, E., Fong, W., Miller, G., Jr & Ryan, P. (1970). Critical obstruction of prosthetic heart valves due to lipid absorption by silastic, *J Thorac Cardiovasc Surg,* Vol. 59 No. 3, pp. 413-425.

Mensing, G., Pearce, T. & Beebe, D.J. (2005). An ultrarapid method of creating 3d channels and microstructures, *Journal of Laboratory Automation,* Vol. 10 No. 1, pp. 24-28.

Mercanzini, A., Cheung, K., Buhl, D.L., Boers, M., Maillard, A., Colin, P., Bensadoun, J.-C., Bertsch, A. & Renaud, P. (2008). Demonstration of cortical recording using novel flexible polymer neural probes, *Sensors and Actuators A: Physical,* Vol. 143 No. 1, pp. 90-96.

Merrill, D.R. (2010). The electrochemistry of charge injection at the electrode/tissue interface, in Zhou, D. & Greenbaum, E. (Eds.), *Implantable neural prostheses 2*. Springer New York, 978-0-387-98120-8, pp. 85-138.

Merrill, D.R., Bikson, M. & Jefferys, J.G.R. (2005). Electrical stimulation of excitable tissue: Design of efficacious and safe protocols, *Journal of Neuroscience Methods,* Vol. 141 No. 2, pp. 171-198.

Metz, S., Bertsch, A., Bertrand, D. & Renaud, P. (2004). Flexible polyimide probes with microelectrodes and embedded microfluidic channels for simultaneous drug delivery and multi-channel monitoring of bioelectric activity, *Biosens Bioelectron,* Vol. 19 No. 10, pp. 1309-1318.

Milliken and Company (1997). Zelec (r) ecp electroconductive powders: Product overview, Available from http://www.zelec-ecp.com/domino/milliken/zelec/zelec.nsf/files/ECPoverview.html

Morin, F., Nishimura, N., Griscom, L., Lepioufle, B., Fujita, H., Takamura, Y. & Tamiya, E. (2006). Constraining the connectivity of neuronal networks cultured on microelectrode arrays with microfluidic techniques: A step towards neuron-based functional chips, *Biosensors and Bioelectronics,* Vol. 21 No. 7, pp. 1093-1100.

Morin, F.O., Takamura, Y. & Tamiya, E. (2005). Investigating neuronal activity with planar microelectrode arrays: Achievements and new perspectives, *J Biosci Bioeng,* Vol. 100 No. 2, pp. 131-143.

Musick, K., Khatami, D. & Wheeler, B.C. (2009). Three-dimensional micro-electrode array for recording dissociated neuronal cultures, *Lab on a Chip,* Vol. 9 No. 14, pp. 2036-2042.

Musienko, P., Van Den Brand, R., Maerzendorfer, O., Larmagnac, A. & Courtine, G. (2009). Combinatory electrical and pharmacological neuroprosthetic interfaces to regain motor function after spinal cord injury, *Biomedical Engineering, IEEE Transactions on,* Vol. 56 No. 11, pp. 2707-2711.

Mussa-Ivaldi, S., Alford, S.T., Chiappalone, M., Fadiga, L., Karniel, A., Kositsky, M., Maggiolini, E., Panzeri, S., Sanguineti, V., Semprini, M. & Vato, A. (2010). New perspectives on the dialogue between brains and machines, *Frontiers in Neuroscience,* Vol. 5, pp. 5.

Myllymaa, S., Myllymaa, K. & Lappalainen, R. (2009). Flexible implantable thin film neural electrodes, in Naik, G.R. (Ed.), *Recent advances in biomedical engineering*. InTech, ISBN: 978-953-307-004-9, Available from: http://www.intechopen.com/articles/show/title/flexible-implantable-thin-film-neural-electrodes, pp. 165-190.

Navarro, X., Krueger, T.B., Lago, N., Micera, S., Stieglitz, T. & Dario, P. (2005). A critical review of interfaces with the peripheral nervous system for the control of neuroprostheses and hybrid bionic systems, *Journal of the Peripheral Nervous System,* Vol. 10 No. 3, pp. 229-258.

Nisch, W., Bock, J., Egert, U., Hammerle, H. & Mohr, A. (1994). A thin film microelectrode array for monitoring extracellular neuronal activity in vitro, *Biosensors & Bioelectronics,* Vol. 9 No. 9-10, pp. 737-741.

Niu, X.Z., Peng, S.L., Liu, L.Y., Wen, W.J. & Sheng, P. (2007). Characterizing and patterning of pdms-based conducting composites, *Advanced Materials,* Vol. 19 No. 18, pp. 2682-2682.

Novak, J.L. & Wheeler, B.C. (1986). Recording from the aplysia abdominal ganglion with a planar microelectrode array, *Biomedical Engineering, IEEE Transactions on,* Vol. BME-33 No. 2, pp. 196-202.

Novak, J.L. & Wheeler, B.C. (1988). Multisite hippocampal slice recording and stimulation using a 32 element microelectrode array, *Journal of Neuroscience Methods,* Vol. 23 No. 2, pp. 149-159.

Offenhausser, A. & Knoll, W. (2001). Cell-transistor hybrid systems and their potential applications, *Trends in Biotechnology,* Vol. 19 No. 2, pp. 62-66.

Offenhäusser, A., Sprossler, C., Matsuzawa, M. & Knoll, W. (1997). Field-effect transistor array for monitoring electrical activity from mammalian neurons in culture, *Biosensors & Bioelectronics,* Vol. 12, pp. 819-826.

Oka, H., Shimono, K., Ogawa, R., Sugihara, H. & Taketani, M. (1999). A new planar multielectrode array for extracellular recording: Application to hippocampal acute slice, *Journal of Neuroscience Methods,* Vol. 93 No. 1, pp. 61-67.

Owens, R.M. & Malliaras, G.G. (2010). Organic electronics at the interface with biology, *Mrs Bulletin,* Vol. 35 No. 6, pp. 449-456.

Pancrazio, J.J., Bey, R.P., Jr., Loloee, A., Manne, S., Chao, H.C., Howard, L.L., Milton-Gosney, W., Borkholder, D.A., Kovacs, G.T.A., Manos, P., Cuttino, D.S. & Stenger, D.A. (1998). Description and demonstration of a cmos amplifier-based-system with measurement and stimulation capability for bioelectrical signal transduction, *Biosensors-&-Bioelectronics,* Vol. 13 No. 9, pp. 971-979.

Park, J., Seyeoul, K., Seung Ik, J., Mcknight, T.E., Melechko, A.V., Simpson, M.L., Dhindsa, M., Heikenfeld, J. & Rack, P.D. (2009). Active-matrix microelectrode arrays integrated with vertically aligned carbon nanofibers, *Electron Device Letters, IEEE,* Vol. 30 No. 3, pp. 254-257.

Patrick, E., Ordonez, M., Alba, N., Sanchez, J.C. & Nishida, T. (2006). Design and fabrication of a flexible substrate microelectrode array for brain machine interfaces, *Conference Proceedings, Annual International Conference of the IEEE Engineering in Medicine and Biology Society,* Vol. 1, pp. 2966-2969.

Pavesi, A., Piraino, F., Fiore, G.B., Farino, K.M., Moretti, M. & Rasponi, M. (2011). How to embed three-dimensional flexible electrodes in microfluidic devices for cell culture applications, *Lab on a Chip,* Vol. advance publication.

Patolsky, F., Timko, B.P., Yu, G., Fang, Y., Greytak, A.B., Zheng, G. & Lieber, C.M. (2006). Detection, stimulation, and inhibition of neuronal signals with high-density nanowire transistor arrays, *Science,* Vol. 313 No. 5790, pp. 1100-1104.

Peppas, N.A., Hilt, J.Z., Khademhosseini, A. & Langer, R. (2006). Hydrogels in biology and medicine: From molecular principles to bionanotechnology, *Advanced Materials,* Vol. 18 No. 11, pp. 1345-1360.

Pine, J. (1980). Recording action potentials from cultured neurons with extracellular microcircuit electrodes, *Journal of Neuroscience Methods,* Vol. 2 No. 1, pp. 19-31.

Pine, J. (2006). A history of mea development, in Taketani, M. & Baudry, M. (Eds.), *Advances in network electrophysiology. Using multi-electrode arrays.* Springer, 978-0-387-25857-7 (Print) 978-0-387-25858-4 (Online), New York, pp. 3-23.

Poghossian, A., Ingebrandt, S., Offenhausser, A. & Schoning, M.J. (2009). Field-effect devices for detecting cellular signals, *Seminars in Cell & Developmental Biology,* Vol. 20 No. 1, pp. 41-48.

Pui, T.-S., Agarwal, A., Ye, F., Balasubramanian, N. & Chen, P. (2009). Cmos-compatible nanowire sensor arrays for detection of cellular bioelectricity, *Small,* Vol. 5 No. 2, pp. 208-212.

Rabaey, K. & Rozendal, R.A. (2010). Microbial electrosynthesis — revisiting the electrical route for microbial production, *Nat Rev Micro,* Vol. 8 No. 10, pp. 706-716.

Rajaraman, S., Choi, S.-O., Shafer, R.H., Ross, J.D., Vukasinovic, J., Choi, Y., Deweerth, S.P., Glezer, A. & Allen, M.G. (2007). Microfabrication technologies for a coupled three-dimensional microelectrode, microfluidic array, *J. Micromech. Microeng.,* Vol. 17 No. 1, pp. 163-171.

Rajaraman, S., Choi, S.O., Mcclain, M.A., Ross, J.D., Laplaca, M.C. & Allen, M.G. (2011). Metal-transfer-micromolded three-dimensional microelectrode arrays for in-vitro brain-slice recordings, *Microelectromechanical Systems, Journal of,* Vol. PP No. 99, pp. 1-14.

Ravichandran, R., Sundarrajan, S., Venugopal, J.R., Mukherjee, S. & Ramakrishna, S. (2010). Applications of conducting polymers and their issues in biomedical engineering, *Journal of the Royal Society Interface,* Vol. 7, pp. S559-S579.

Rodger, D.C., Fong, A.J., Li, W., Ameri, H., Ahuja, A.K., Gutierrez, C., Lavrov, I., Zhong, H., Menon, P.R., Meng, E., Burdick, J.W., Roy, R.R., Edgerton, V.R., Weiland, J.D., Humayun, M.S. & Tai, Y.-C. (2008). Flexible parylene-based multielectrode array technology for high-density neural stimulation and recording, *Sensors and Actuators, B: Chemical,* Vol. 132 No. 2, pp. 449-460.

Rogers, J.A., Someya, T. & Huang, Y. (2010). Materials and mechanics for stretchable electronics, *Science,* Vol. 327 No. 5973, pp. 1603-1607.

Ross, J., Brown, E.A., Rajaraman, S., Allen, M.G. & Wheeler, B. (2010). Apparatus and methods for high throughput network electrophysiology and cellular analysis, in, ISBN, USA.

Rothschild, R.M. (2010). Neuroengineering tools/applications for bidirectional interfaces, brain computer interfaces, and neuroprosthetic implants - a review of recent progress, *Frontiers in Neuroengineering,* Vol. 4, pp. 12.

Rozlosnik, N. (2009). New directions in medical biosensors employing poly(3,4-ethylenedioxy thiophene) derivative-based electrodes, *Analytical and Bioanalytical Chemistry,* Vol. 395 No. 3, pp. 637-645.

Rutledge, L.T. & Duncan, J.A. (1966). Extracellular recording of converging input on cortical neurones using a flexible microelectrode, *Nature,* Vol. 210 No. 5037, pp. 737-739.

Rutten, W.L.C. (2002). Selective electrical interfaces with the nervous system, *Annual Review of Biomedical Engineering,* Vol. 4 No. 1, pp. 407-452.

Ryynänen, T., Kujala, V., Ylä-Outinen, L., Kerkelä, E., Narkilahti, S. & Lekkala, J. (2010). Polystyrene coated mea, in Stett, A. (Ed.), *Proceedings of the 7th Int. Meeting on Substrate-Integrated Microelectrode Arrays, June 29 – July 2*. BIOPRO Baden-Württemberg GmbH, ISBN, Reutlingen, pp. 265-266.

Sadleir, R.J., Grant, S.C., Demarse, T.B., Woo, E.J., Lee, S.Y., Kim, T.S., Oh, S.H., Lee, B.I. & Seo, J.K. (2005). Study of mri/mea compatibility at 17.6 tesla, *International Journal of Bioelectromagnetism,* Vol. 7 No. 1, pp. 278-281.

Sandison, M., Curtis, A.S.G. & Wilkinson, C.D.W. (2002). Effective extra-cellular recording from vertebrate neurons in culture using a new type of micro-electrode array, *Journal of Neuroscience Methods,* Vol. 114 No. 1, pp. 63-71.

Schmidt, C.E., Shastri, V.R., Vacanti, J.P. & Langer, R. (1997). Stimulation of neurite outgrowth using an electrically conducting polymer, *Proceedings of the National Academy of Sciences of the United States of America,* Vol. 94 No. 17, pp. 8948-8953.

Seidl, K. & *Et al.* (2010). In-plane silicon probes for simultaneous neural recording and drug delivery, *Journal of Micromechanics and Microengineering,* Vol. 20 No. 10, pp. 105006.

Sekitani, T., Nakajima, H., Maeda, H., Fukushima, T., Aida, T., Hata, K. & Someya, T. (2009). Stretchable active-matrix organic light-emitting diode display using printable elastic conductors, *Nature Materials,* Vol. 8 No. 6, pp. 494-499.

Sirivisoot, S., Pareta, R. & Webster, T.J. (2011). Electrically controlled drug release from nanostructured polypyrrole coated on titanium, *Nanotechnology,* Vol. 22 No. 8, pp. 085101.

Smoothon, I. (2008). Smooth-sil® platinum cure silicone rubber (technical bulletin), in, ISBN.

Starovoytov, A., Choi, J. & Seung, H.S. (2005). Light-directed electrical stimulation of neurons cultured on silicon wafers, *J Neurophysiol,* Vol. 93 No. 2, pp. 1090-1098.

Stein, B., George, M., Gaub, H.E. & Parak, W.J. (2004). Extracellular measurements of averaged ionic currents with the light-addressable potentiometric sensor (laps), *Sensors and Actuators B: Chemical,* Vol. 98 No. 2-3, pp. 299-304.

Stieglitz, T., Rubehn, B., Henle, C., Kisban, S., Herwik, S., Ruther, P. & Schuettler, M. (2009). Brain-computer interfaces: An overview of the hardware to record neural signals from the cortex, in Verhaagen, J., Hol, E.M., Huitenga, I., Wijnholds, J.,

Bergen, A.B., Boer, G.J. & Dick, F.S. (Eds.), *Progress in brain research*. Elsevier, 0079-6123, pp. 297-315.

Stoppini, L., Duport, S. & Correges, P. (1997). A new extracellular multirecording system for electrophysiological studies: Application to hippocampal organotypic cultures, *Journal of Neuroscience Methods,* Vol. 72 No. 1, pp. 23-33.

Suzuki, T., Ziegler, D., Mabuchi, K. & Takeuchi, S. (2004). Flexible neural probes with micro-fluidic channels for stable interface with the nervous system, in *Engineering in Medicine and Biology Society, 2004. IEMBS '04. 26th Annual International Conference of the IEEE*, ISBN, pp. 4057-4058.

Suzurikawa, J., Takahashi, H., Takayama, Y., Warisawa, S., Mitsuishi, M., Nakao, M. & Jimbo, Y. (2006). Light-addressable planar electrode with hydrogenated amorphous silicon and low-conductive passivation layer for stimulation of cultured neurons, in *Engineering in Medicine and Biology Society, 2006. EMBS '06. 28th Annual International Conference of the IEEE*, ISBN, pp. 648-651.

Svennersten, K., Larsson, K.C., Berggren, M. & Richter-Dahlfors, A. (2011). Organic bioelectronics in nanomedicine, *Biochimica et Biophysica Acta (BBA) - General Subjects,* Vol. 1810 No. 3, pp. 276-285.

Thiebaud, P., Beuret, C., Koudelka-Hep, M., Bove, M., Martinoia, S., Grattarola, M., Jahnsen, H., Rebaudo, R., Balestrino, M., Zimmer, J. & Dupont, Y. (1999). An array of pt-tip microelectrodes for extracellular monitoring of activity of brain slices, *Biosensors & Bioelectronics,* Vol. 14 No. 1, pp. 61-65.

Thiébaud, P., De Rooij, N.F., Koudelka-Hepp, M. & Stoppini, L. (1997). Microelectrode arrays for electrophysiological monitoring of hippocampal organotypic slice cultures, *IEEE Transactions on Biomedical Engineering,* Vol. 44 No. 11, pp. 1159-1163.

Thiel, M., Fischer, J., Von Freymann, G. & Wegener, M. (2010). Direct laser writing of three-dimensional submicron structures using a continuous-wave laser at 532 nm, *Applied Physics Letters,* Vol. 97 No. 22, pp. 221102-221103.

Thomas, C.A., Springer, P.A., Loeb, G.E., Berwald-Netter, Y. & Okun, L.M. (1972). A miniature microelectrode array to monitor the bioelectric activity of cultured cells, *Experimental Cell Research,* Vol. 74, pp. 61-66.

Thompson, B.C., Richardson, R.T., Moulton, S.E., Evans, A.J., O'leary, S., Clark, G.M. & Wallace, G.G. (2010). Conducting polymers, dual neurotrophins and pulsed electrical stimulation - dramatic effects on neurite outgrowth, *Journal of Controlled Release,* Vol. 141 No. 2, pp. 161-167.

Tian, B., Cohen-Karni, T., Qing, Q., Duan, X., Xie, P. & Lieber, C.M. (2010). Three-dimensional, flexible nanoscale field-effect transistors as localized bioprobes, *Science,* Vol. 329 No. 5993, pp. 830-834.

Tonomura, W., Moriguchi, H., Jimbo, Y. & Konishi, S. (2010). Parallel multipoint recording of aligned and cultured neurons on micro channel array toward cellular network analysis, *Biomedical Microdevices,* Vol. 12 No. 4, pp. 737-743.

Volta, A. (1793). *Schriften über die thierische elektrizität* Johann Mayer, Prag.

Wang, T., Yang, W., Huang, H. & Fu, C. (2007). A novel fabrication method of flexible micro electrode array for neural recording, in *Micro Electro Mechanical Systems, 2007. MEMS. IEEE 20th International Conference on*, ISBN, pp. 295-300.

Wei, P., Taylor, R., Ding, Z., Higgs, G., Norman, J.J., Pruitt, B.L. & Ziaie, B. (2009). A stretchable cell culture platform with embedded electrode array, in *Micro Electro Mechanical Systems, 2009. MEMS 2009. IEEE 22nd International Conference on*, ISBN, pp. 407-410.

Widge, A.S., Jeffries-El, M., Cui, X., Lagenaur, C.F. & Matsuoka, Y. (2007). Self-assembled monolayers of polythiophene conductive polymers improve biocompatibility and electrical impedance of neural electrodes, *Biosens Bioelectron,* Vol. 22 No. 8, pp. 1723-1732.

Wilkinson, C.D. (2004). Making structures for cell engineering, *Eur Cell Mater,* Vol. 8, pp. 21-25; discussion 25-26.

Wilks, S.J., Richardson-Burns, S.M., Hendricks, J.L., Martin, D.C. & Otto, K.J. (2009). Poly(3,4-ethylene dioxythiophene) (pedot) as a micro-neural interface material for electrostimulation, *Frontiers in Neuroengineering,* Vol. 2, pp. 1-8.

Williams, K.R. & Muller, R.S. (1996). Etch rates for micromachining processing, *Microelectromechanical Systems, Journal of,* Vol. 5 No. 4, pp. 256-269.

Winter, J.O., Cogan, S.F. & Rizzo, J.F. (2007). Retinal prostheses: Current challenges and future outlook, *Journal of Biomaterials Science, Polymer Edition,* Vol. 18, pp. 1031-1055.

Wise, K.D., Sodagar, A.M., Ying, Y., Gulari, M.N., Perlin, G.E. & Najafi, K. (2008). *Microelectrodes, microelectronics, and implantable neural microsystems : Progress in development of tiny electrodes, cables, circuitry, signal processors and wireless interfaces promises to advance understanding of the human nervous system and its disorders*, Institute of Electrical and Electronics Engineers, New York, USA.

Wong, J.Y., Langer, R. & Ingber, D.E. (1994). Electrically conducting polymers can noninvasively control the shape and growth of mammalian cells, *Proceedings of the National Academy of Sciences,* Vol. 91 No. 8, pp. 3201-3204.

Xin, Z., Wai Man, W., Yulong, Z., Yandong, Z., Fei, G., Nelson, R.D. & Larue, J.C. (2009). Design of a cmos-based multichannel integrated biosensor chip for bioelectronic interface with neurons, in *Engineering in Medicine and Biology Society, 2009. EMBC 2009. Annual International Conference of the IEEE*, ISBN, pp. 3814-3817.

Yang, J., Kim, D.H., Hendricks, J.L., Leach, M., Northey, R. & Martin, D.C. (2005). Ordered surfactant-templated poly(3,4-ethylenedioxythiophene) (pedot) conducting polymer on microfabricated neural probes, *Acta Biomaterialia,* Vol. 1 No. 1, pp. 125-136.

Yong-Kyu, Y., Jung-Hwan, P. & Allen, M.G. (2006). Multidirectional uv lithography for complex 3-d mems structures, *Microelectromechanical Systems, Journal of,* Vol. 15 No. 5, pp. 1121-1130.

Zhang, M., Wu, J., Wang, L., Xiao, K. & Wen, W. (2010). A simple method for fabricating multi-layer pdms structures for 3d microfluidic chips, *Lab Chip,* Vol. 10 No. 9, pp. 1199-1203.

Zhang, R., Moon, K.-S., Lin, W., Agar, J.C. & Wong, C.-P. (2011). A simple, low-cost approach to prepare flexible highly conductive polymer composites by in situ reduction of silver carboxylate for flexible electronic applications, *Composites Science and Technology,* Vol. 71 No. 4, pp. 528-534.

Zhou, D.D. & Greenberg, R.J. (2009). Microelectronic visual prostheses, in Greenbaum, E. & Zhou, D. (Eds.), *Implantable neural prostheses 1*. Springer New York, 978-0-387-77261-5, pp. 1-42.

Ziaie, B. (2009). Stretchable bioelectrodes, in *Engineering in Medicine and Biology Society, 2009. EMBC 2009. Annual International Conference of the IEEE*, ISBN, pp. 1049-1052.

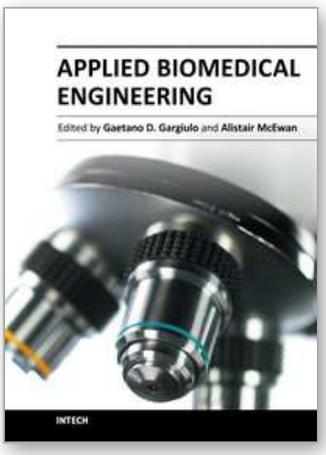

Applied Biomedical Engineering

Edited by Dr. Gaetano Gargiulo

ISBN 978-953-307-256-2
Hard cover, 500 pages
Publisher InTech
Published online 23, August, 2011
Published in print edition August, 2011

This book presents a collection of recent and extended academic works in selected topics of biomedical technology, biomedical instrumentations, biomedical signal processing and bio-imaging. This wide range of topics provide a valuable update to researchers in the multidisciplinary area of biomedical engineering and an interesting introduction for engineers new to the area. The techniques covered include modelling, experimentation and discussion with the application areas ranging from bio-sensors development to neurophysiology, telemedicine and biomedical signal classification.

INTECH
open science | open minds

InTech Europe
University Campus STeP Ri
Slavka Krautzeka 83/A
51000 Rijeka, Croatia
Phone: +385 (51) 770 447
Fax: +385 (51) 686 166
www.intechopen.com

InTech China
Unit 405, Office Block, Hotel Equatorial Shanghai
No.65, Yan An Road (West), Shanghai, 200040, China
中国上海市延安西路65号上海国际贵都大饭店办公楼405单元
Phone: +86-21-62489820
Fax: +86-21-62489821

IntechOpen